Preparation and Characterization of Bio-based PCM Microcapsules for Thermal Energy Storage

Maryam Fashandi

A THESIS SUBMITTED TO THE FACULTY OF GRADUATE STUDIES
IN PARTIAL FULFILLMENT OF THE REQUIREMENTS FOR THE
DEGREE OF MASTER OF APPLIED SCIENCE

Graduate Program in

Mechanical Engineering

York University

Toronto, Ontario

October 2017

Abstract

Phase change materials (PCM) have gained extensive attention in thermal energy storage applications. During their phase transition, the energy can be stored in or released from PCM. While changing from solid state to liquid state, PCM start to flow. Encapsulation is a widely-used technique to prevent PCM from migrating and reacting with their environment. In the first phase of the thesis, microencapsulation of 100% bio-based (organic) PCM microcapsules by solvent evaporation and oil-in-water emulsification was investigated under different conditions, resulting in optimal properties. For the second phase, the focus was on the studies of inorganic PCM, which have higher latent heat of melting, higher thermal conductivity and lower price than the organic PCM. However, their supercooling, phase segregation, and hydrophilic nature have caused major challenges to their applications. Tuning the thermal properties, including crystallization temperature and phase segregation of inorganic PCM by using bio-based nanoparticles and other additives was investigated in the second part of the research. Due to the hydrophilic nature of the inorganic PCM, a double emulsion (water in oil in water) solvent evaporation technique was explored for encapsulation with a polymeric shell. The challenges and strategies for supercooling prevention and encapsulating the hydrophilic PCM were investigated.

Acknowledgements

I should use this opportunity to thank everyone who supported me through my master's studies at York University and show my gratitude towards them.

I would like to express my sincere gratitude toward my supervisor Professor Sunny Leung, first for his knowledge, patience, and support, second for his encouragement whenever the research became difficult and third for giving me the great opportunity of studying in Canada. I have been extremely lucky to have such a great supervisor.

I should express my deepest thanks to my advisory committee, Dr. Magdalene Krol and Dr. Eldyasti from civil engineering department and Dr. Paul O'Brien from mechanical engineering department, for reviewing this manuscript and giving me feedbacks on my final oral examination. I extend my gratitude to all the professors and staff in mechanical engineering department, especially Ms. Ruth Milton and Ms. Carianne Hathaway, for their kindness and support. Also, I should thank York University and faculty of graduate studies for providing academic funding.

I would like to especially thank Dr. Yanting Guo, for her infinite support, wisdom, and help during my studies at York University. I would also extend my appreciation to all my friends in Lassonde School of Engineering, York University for their friendship. My gratitude also goes to my friends in Iran, for their great support and proving that thousands of miles of distance could not affect our friendship.

I should express my deep sense of gratitude to my father, Reza Fashandi, for his wisdom, support, and love. Last but not least, I must thank my wonderful sisters, Homa and Faeze, for

their love, support, understanding, and motivation. I could not finish my studies without their help.

I dedicate this thesis to the bright memory of mother, Forough Mallak. Although she left this world before I enter university, her enthusiasm for learning has been the greatest motivation for me throughout my studies.

Table of Contents

List of Tables

List of Figures

List of Abbreviations

BA	butyl acrylate
BMA	butyl methacrylate
CMC	carboxymethyl cellulose
CMC	critical micelle concentration
CNT	carbon nanotube
CNW	chitin nanowhisker
CTAB	cetyl trimethylammonium bromide
DCM	dichloromethane
DE	double emulsion
DI	deionized
DSC	differential scanning calorimetry
DVB	divinylbenzene
EDA	ethylene diamine
FTIR	Fourier transform infrared
GNP	graphene nanoplatelets
GO	graphene oxide
hBN	hexagonal boron nitride
HIPS	high-impact polystyrene
HLB	hydrophile-lyophile balance
HVAC	heating, ventilation, and air conditioning
IPDI	isophorone diisocyanate
LA	lauric acid
MA	myristic acid
MMA	methyl methacrylate
PA	palmitic acid
PBA	poly(butyl acrylate)
PBMA	poly(butyl methacrylate)
PCL	polycaprolactone

PCM	phase change material
PEG	polyethylene glycol
PETA	pentaerythritol triacrylate
PLA	polylactic acid
PLGA	poly(lactic-co-glycolic acid)
PMMA	poly(methyl methacrylate)
PVA	polyvinyl alcohol
PVP	polyvinylpyrrolidone
o/w	oil in water
s/o/w	solid in oil in water
SA	stearic acid
SAT	sodium acetate trihydrate
SDBS	sodium dodecyl benzenesulfonate
SDS	sodium dodecyl sulfate
SEM	scanning electron microscopy
St	styrene
TES	thermal energy storage
TGA	thermogravimetric analysis
USD	United States dollar
w/o/w	water in oil in water

Chapter 1
Preamble

1.1. Introduction

Planet Earth has experienced different periods of extreme cooling and warming since its birth due to natural causes such as volcanos or differences in the sun's output. However, today's extreme rise in average temperature of the earth is largely caused by human's industrial activities, which has led to severe increases in greenhouse gas emissions [1]. Carbon dioxide and water vapor are the main types of greenhouse gases. Green house gas effect is due to thermal radiation from earth being absorbed by CO_2 and H_2O in the atmosphere [2]. They are the main causes of global warming and scientists have predicted that by the end of twenty-first century, the average temperature of the Earth can rise by up to 7 °C [3].

It has been reported that in 2010, 38% of all carbon dioxide emission was due to electricity and heat generation by using fossil fuels [4]. Each stage of extracting, refining, distributing and consuming fossil fuels has caused many problems not only for human health but also for the entire ecosystem. Water and air pollution, land degradation, as well as political crises due to the unbalanced distribution of fossil fuel resources are only a few devastating consequences of extensive consumption of fossil fuels [5]. Reduction in energy consumption and improvement in energy preservation systems represent reasonable ways to suppresse greenhouse gas emissions and thereby reduce the rate of global warming. Although one cannot claim that using renewable energy can completely solve the problem, a wide search for alternatives to fossil fuels has been started for years and is continuing [6].

In this context, the uses of phase change materials (PCM) to store thermal energy is one potential solution that can help reduce the need of using fossil fuels. During their phase transition (i.e., solid-liquid, solid–gas or liquid–gas), latent heat will be stored in or released from PCM [7]. When PCM undergo isothermal melting, sublimation or vaporization, heat is absorbed from the surrounding and stored in them. In contrast, when PCM solidify or condense, energy is released. Due to their wide range of melting points, different PCM are suitable for thermal energy storage applications under diverse circumstances. Although PCM undergoing liquid-gas transition have higher heat storage capacity than those undergoing solid-liquid transition, the latter have higher practicality because of their smaller volume changes in comparison to PCM that undergo a liquid-gas transition [8,9].

PCM can be classified as organic PCM, inorganic PCM, and eutectics. The amount of thermal energy that can be stored in inorganic PCM, like salts, salt hydrates, metals, and alloys, are up to two times that can be stored in organic ones. They are also nonflammable as well as are less expensive and more thermally conductive than organic PCM. However, their corrosiveness, as well as supercooling behaviors, have limited their applications [10]. Supercooling brings randomness to the storing and releasing cycles and hence is not favorable. Organic PCM can be subdivided into paraffinic and non-paraffinic materials. Paraffinic petroleum-based PCM are the most commonly used PCM. They possess respectable amount of latent heat. They also have limited supercooling, no corrosiveness, good thermal and mechanical stability, low vapor pressure, as well as self-nucleating ability. However, their drawbacks include low thermal conductivity, flammability, and being more expensive than inorganic PCM [8,11]. Non-paraffinic PCM are mostly bio-derived from vegetable oil (e.g., soybean oil, coconut oil, palm oil, etc.). Furthermore, fatty acids, esters, alcohols and glycols are some well-known examples of

this sub-category of PCM [12]. By covering a wide range of melting temperatures, these bio-based PCM are appropriate candidates for thermal energy storage applications in different environments. Eutectics are a mixture of two or more PCM together. These mixtures can be made of inorganic PCM with inorganic PCM, organic PCM with inorganic PCM, and organic PCM with organic PCM. The final melting points of the eutectics are lower than any of the individual PCM [13].

When PCM undergo a phase transition from a solid states to a liquid state, they start to flow and they can contaminate and react with the surrounding area. In this context, encapsulation is a widely-used technique to prevent PCM from migrating and reacting with their environment. The PCM encapsulated by any shell in the micron size is called microPCM.

1.2. Research goals and objectives

The overarching goal of this thesis research is to prepare PCM microcapsules with increased environmental sustainability for thermal energy storage. For this reason, two main types of PCM (i.e. organic and inorganic) were used. In the first phase of the research, 100% bio-based PCM microcapsules were prepared through a single emulsion (i.e., oil in water) solvent evaporation method. The effects of different parameters on the properties of the microPCM were investigated.

The second phase of the research focused on the uses of inorganic PCM for thermal energy storage, and is subdivided into two sub-phases (i.e., 2a and 2b). In phase 2a, the effects of bio-based nanoparticles and other additives on the prevention of supercooling and phase segregation were explored. Phase 2b investigated the encapsulation of the hydrophilic salt hydrate with a bio-based polymer using a double emulsion (i.e., water in oil in water) solvent evaporation technique.

1.3. Thesis structure

This thesis contains five chapters. Chapter one describes the critical climatic situation of the earth. It explains the necessity of finding alternative ways to reduce the usage of fossil fuels and using phase change materials for thermal energy storage applications, as well as the goals and objectives of this research. Chapter 2 provides a comprehensive literature survey and review on the background of the research. Chapters 3 and 4 introduce the phases of the research. In Chapter 3, the preparation and characterization of palmitic acid as a bio-based organic PCM with bio-based polylactic acid (PLA) shell is investigated. Chapter 4 describes the supercooling prevention of sodium acetate trihydrate (SAT) as an inorganic PCM nanocomposite and encapsulation of this hydrophilic salt in PLA. Finally, Chapter 5 concludes the contribution of this thesis and provides some potential future directions of this research.

Chapter 2
Background and Literature Review

2.1. PCM

Phase Change Materials (PCM) are a class of materials that can store energy as latent heat. The energy is stored in or released from them when they undergo phase transition. The transition can be in the form of solid-liquid, solid-solid, solid-gas or liquid-gas. During the phase transition, the energy will be stored in or released from PCM [3]. When PCM undergo isothermal melting, sublimation or vaporization, energy is absorbed from the surrounding and stored in the material. In contrast, when PCM solidify or condense, energy is released [14].

Their wide range of melting points have made them suitable for diverse applications. The temperature range can be from subzero temperatures up to hundreds of degrees. Moreover, they possess acceptable heat storage capacity from 100 up to 400 $J \cdot g^{-1}$[8]. Among all types of PCM undergoing different routes of phase transition, solid-liquid PCM have the highest usage rate. Although liquid-gas PCM also have high heat capacity, the large volume change during their transitions from liquid phase to gas phase have limited their applications. In contrast, solid-liquid PCM undergo a lower degree of volume change during the process of phase transition, making them more practical for applications. Nevertheless, their abilities to flow in their liquid states still cause problem in applications. In this context, encapsulation is a proper technique to prevent the leakage of PCM during phase transition. Furthermore, preparation of PCM capsules with a sizr on the order of microns would also enhance the heat transfer between PCM and their surrounding [15], leading to higher rates of energy storage and release during their operations.

Solid-solid PCM are another class of thermal energy storage materials. The storage and release of energy is associated with the changes in their crystalline structures. Compared to other classes of PCM, they have superior properties such as low volume change during phase transition and no leakage. Therefore, this class of PCM do not need to be encapsulated. However, their storage capacity is lower than other PCM [8,16]. In general, two methods have been used to manufacture solid-solid PCM. One is a physical method and the other is a chemical method. In the physical method, PCM is first dispersed in a polymeric matrix. The matrix should have a higher melting point than the PCM and it acts as a supporting material. When the PCM undergoes a phase transition, the polymer will keep its shape hence this kind of solid-solid PCM is called shape-stabilized or form-stable PCM. However, this type of PCM has shown instability and phase segregation after multiple melting and freezing cycles [17]. In the chemical method, the PCM is bonded to the polymer matrix by means of crosslinking, grafting or copolymerization. This prohibits the flowing of PCM at temperatures above their melting points [18].

This chapter starts by discussing the performances of different classes of PCM. It is followed by reviewing various encapsulation techniques investigated in pervious researches. The chapter is concluded by a comprehensive review of recent researches related to the PCM technology.

2.2. Classification of phase change materials

PCM are generally classified as organic, inorganic and eutectics. Organic PCM are subdivided into paraffinic and non-paraffinic materials.

2.2.1. Organic PCM (Paraffinic)

Alkanes or paraffin are a group of acrylic saturated hydrocarbon that have a general chemical formula of C_nH_{2n+2}. Both their boiling points and melting points increase with a higher number

of carbon atoms in their backbones [19]. Alkanes with one to four carbon atoms are gases under ambient conditions. In contrast, those containing 5 to 17 carbons in their main chains are liquid while paraffin with 18 or more carbons atoms are solid at room temperature [20]. Their advantages in thermal energy storage applications include high latent heat, negligible supercooling, no reactivity, good thermal and mechanical stability, low vapor pressure, and self-nucleating behavior. However, they suffer from low thermal conductivity and high flammability [8,11]. With the aforementioned advantages, organic PCM are the most commonly used PCM although their prices are higher than salt hydrates [21]. Many researchers have investigated the thermal stability of different kinds of paraffin, and it has been revealed that the melting point and enthalpy of fusion remain virtually unchanged after 600 to 1500 heating and cooling cycles [22,23]. The blend of pure alkanes, which is a molecular alloy, can extend the temperature range of PCM to lower temperatures. It is because the alloy has a lower melting point than all of the components and make them suitable for more diverse applications. The molecular alloy is considered to be a eutectic, which will be discussed in later parts of this chapter. Paraffin wax, which is a by-product of crude oil and a mixture of different alkanes, is another commonly used PCM due to its abundance and lower price [12,24]. In the literature, a paraffin wax is not considered as a eutectic. However, if this wax is mixed with other PCM, it is considered as a eutectic.

2.2.2. Organic PCM (non-Paraffinic)

Non-paraffinic PCM are mostly derived from vegetable oil (e.g., soybean oil, coconut oil, palm oil, etc). Their melting points cover a wide range of temperatures, which made them suitable for many applications. Similar to conventional paraffinic PCM, their advantages include high latent heat, low vapor pressure, good chemical and thermal stability, self-nucleating

behavior and high abundance. In addition, these bio-based PCM are less flammable than paraffinic ones. This makes them a better choice for many applications, especially for construction and building materials [25]. The most well-known bio-based PCM are alcohols, ester, fatty acids, and glycols [13]. Thermal cycling results have demonstrated that this class of PCM possess very good thermal stability [12]. However, one drawback of fatty acids is their corrosiveness when they are in contact with metals [26].

2.2.3. Inorganic PCM

Inorganic PCM consists of metals, alloys, and salt hydrates. Their benefits over organic PCM include higher latent heat, higher thermal conductivity and lower cost. Most Metallic PCM have a melting point above 300°C, which makes them suitable for solar power plants uses [27]. Alloy PCM are a binary or ternary mixture of metals that show a high thermal conductivity like the metal PCM. This will eliminate the need to add thermally conductive filler to the PCM [10]. Salt hydrates are generally represented by a chemical formula in the form of $A_xB_y \cdot n(H_2O)$, where n represents the number of H_2O molecules associated with the salt structure; and A_xB_y shows metal carbonate, sulfite, phosphate, nitrite, acetate, or chloride. They show corrosiveness when they are in contact with metals, which limits their long-term applications. Furthermore, supercooling and phase segregation are other disadvantages of salt hydrates. Unlike salt hydrates, metal and metallic alloy PCM do not suffer from these disadvantages.

Phase segregation happens when two macroscopic phases (e.g., water phase and salt phase) are formed during repeated heating and cooling cycles due to the difference in their densities. The phase separation can be avoided using a thickening agent. By making a fine network and enhancing the viscosity of a salt hydrate, the thickening agent can avoid the phase separation of the salt and water part of the PCM [28]. In the literature, Ryu *et al.* [29] observed that a super

absorbent polymer made from acrylic based polymers can be effective in phase segregation prevention of the materials with a high number (i.e., 10 to 12) of hydrates, and carboxymethyl cellulose (CMC) is effective in avoiding the phase segregation of salts with a low number (i.e., 3 to 5) of hydrates. Mao *et al.* [30] prepared sodium acetate trihydrate (SAT) composites using three different nucleating agents (i.e., gelatin, CMC and polyacrylamide) and they managed to observe a phase transition using CMC and gelatin. Polyvinyl alcohol, silica gel, and sepiolite are other chemicals that have been used as the thickening agent [31].

Supercooling phenomenon does not necessarily mean that the salt hydrate is unable to nucleate and subsequently initiate crystallization. Sometimes the salt hydrate does produce the nuclei. However, their sizes cannot reach the critical level required for crystallization. Crystal nucleation can be subdivided into homogeneous and heterogeneous nucleation. For homogenous nucleation, the material does not need any external factor to initiate crystallization. When the temperature of the material reaches the freezing point, it undergoes some density fluctuations. This will in turn assist the formation of nuclei and the initiation of crystallization [32]. Heterogeneous nucleation occurs at the surface of a foreign body such as an external nucleating agent, the surface of the PCM container, impurities, bubbles, etc.

There are two main methods to suppress the supercooling of salt hydrates: (i) cold finger and (ii) addition of external nucleating agents. These methods take advantage of heterogenous nucleation. In the cold finger method, a piece of material (e.g., a glass or a metal tube) is inserted into the PCM container. This material is attached to a cold source (e.g., flow of the liquid argon inside the cold finger tube), which provides a local low temperature region that can initiate nucleation in the bulk of the PCM [33,34]. Nucleating agents are external materials with melting points higher than that of the PCM. As a result, they can remain in their solid states when the

PCM store thermal energy during their melting cycle. Appropriate nucleating agents should have stable physical and chemical properties; otherwise, they cannot ensure consistent performances of the salt hydrates over repeating heating-cooling cycles during their operations [35].

Three main types of nucleating agent's crystal structure are: (i) isomorphous, (ii) isotypic and (iii) epitaxial. The first two groups have similar crystal structures to the PCM and the isotypic agents, in particular, also have a similar chemical structure to the PCM. Epitaxial nucleating agent do not have any similarity with either the chemical or the crystal structure of the PCM. The reason behind their effectiveness in supercooling prevention of salt hydrates is still unknown [36,37].

Different nucleating agents have been used to prevent the supercooling of salt hydrates. Hu *et al.* [38] added 5 wt.% of aluminium nitride and 4 wt.% of CMC to SAT as the nucleating agent and thickening agent, respectively. They managed to fully prevent the supercooling in this PCM and simultaneously enhance the dehydration temperature. Cui *et al.* [39] prepared a nanocomposite using SAT, 0.5 wt.% of nano-copper, and 3 wt.% of CMC. The final product did not show any supercooling and its thermal conductivity was enhanced due to the presence of nano-copper. Mao *et al.* [30] used disodium phosphate dodecahydrate as a nucleating agent for SAT and expanded graphite as a thermally conductive filler. The final composite showed almost no supercooling; however, the thermal properties exhibited some deterioration after repeated thermal cycling. This can be attributed to the instability of the nucleating agent used in the composite.

Among all the papers using different nucleating agents for supercooling prevention of salt hydrates, no paper has investigated all the different parameters that can affect the supercooling degree of the salt hydrate. These parameters are salt hydrate particle size, initial heating

temperature, nucleating agent content, surfactant content, and thermally conductive filler content. Moreoever, none of the papers have explored the use of a bio-derived nucleating agent for supercooling prevention purposes.

2.2.4. Eutectic PCM

Eutectics are mixtures of different PCM. The components can be purely organic, purely inorganic, or a combination of organic and inorganic PCM. They can melt and freeze congruently without any phase segregation. The melting point of a eutectic PCM is typically lower than that of each component in the mixture [40]. By using this property, one can make PCM with melting points as low as -62°C [41]. These PCM have been applied in ventilation systems, ski resorts, frozen food protection, transportation, and production of dry ice [41]. By searching through existing literatures, one can realize that most eutectics prepared today are mixtures of two organic PCM. Sari *et al.* have conducted an extensive research on different types of organic PCM eutectics for building materials such as lauric acid/stearic acid (LA/SA), myristic acid/palmitic acid (MA/PA) and palmitic acid/stearic acid (PA/SA). All of these composites went through 360 heating and cooling cycles and their melting point and latent heat of fusion remained unchanged [42]. However, there are few researches focused on combination of different inorganic PCM. As an example, Nagano *et al.* [43] prepared a composite of magnesium chloride hexahydrate and magnesium nitrate hexahydrate with a ratio of 20:80. The melting point and latent heat of fusion of the final product were 60°C and 150 $J \cdot g^{-1}$ respectively. These properties remained almost unchanged after 1000 heating and cooling cycles. It has been revealed that the solidification of this eutectic PCM mixture occurred within 10°C from the freezing point of the fresh composite.

2.3. Encapsulation of phase change materials

PCM undergo a volume change during the process of solid-liquid phase transition. Encapsulation is a proper technique to prevent the leakage due to the fluidity in liquid phase, and increase the area for heat transfer, thereby enhancing the heat transfer rate. The heat transfer rate is higher in micro and nanocapsules, in comparison to macrocapsules [44]. Enhancing heat transfer rate leads to having a shorter duration for charging and discharging of the PCM. In this way, the use of PCM in devices like heat exchangers can be more effective. It should be noted that increasing the heat transfer rate or thermal conductivity of the PCM are not always favorable. PCM has two main applications: thermal protection and thermal energy storage. In the first application, PCM is as an insulating material; therefore, low thermal conductivity is desirable. In heat storage applications like heat exchangers or solar heaters that are embedded with PCM, a high thermal conductivity is required. It is because although sufficient energy is available for charging the PCM, there is not enough time to use it [45].

A proper encapsulating material should meet the requirements of the system such as compatibility with the core material, strength, and flexibility that are needed. It should have the ability to protect the PCM from any external damages. Moreover, it should be chemically safe since it is likely to be in direct contact with consumers. Two methods of encapsulation (i.e., macroencapsulation and microencapsulation), based on the size of the final capsules, have been applied to envelop PCM. Various researches on encapsulation technology of PCM are discussed in this chapter [8,46].

2.3.1. Macroencapsulation of phase change materials

The sizes of macro-capsules are larger than 1 mm. Macroencapsulation is the most commonly used approach in today's PCM packaging. This involves the wrapping of big loads of PCM in a

polymeric pocket, bottle, shell, tube, thin plate, sphere, etc. However, this method has lots of disadvantages in comparison to microencapsulation, such as the possibility of polymeric wrap (or bottle) to be torn and the PCM to leak to the surrounding area, the slow heat transfer rate due to low surface to volume ratio, inflexibility and high volume of the PCM package [47]. Several investigations have been done on the application of PCM macroencapsulation in refrigeration. Fioretti *et al.* [48] included a PCM layer with a melting point of 35°C wrapped in polyethylene panels to a reefer wall and compared the power usage of the container to that of a normal one. They observed that under the same condition, the interior temperature of the reefer is 1-2°C lower than that of the normal container. Cheng *et al.* [49] managed to include the PCM in a condenser and reach to 12% saving in energy consumption. In today's food packaging, macroencapsulated PCM are commonly used in the form of boxes, sheets, sachets or bottles. Metallic containers can be used if high thermal conductivity is needed. In contrast, the uses of microencapsulated PCM films are uncommon in industry. Nevertheless, it is critical to verify the compatibility between the PCM and the container before using them [44].

2.3.2. Microencapsulation of phase change materials

Microencapsulation is defined as wrapping any material in a capsule with a diameter of 1 to 1000 μm. This helps to decrease the chance of damage and increase the heat transfer rate of the PCM microcapsule and its surroundings because of a large surface area to volume ratio. Any capsule with a diameter less than 1 μm is defined as nanocapsule. A research showed that a 10 nm nanocapsule has a higher structural stability than a 10 μm microcapsule with the same ratio of core to shell material. Nanocapsules are less likely to be damaged when flowing or pumping, hence they are more suitable for long-term purposes. However, almost all researches reported encapsulation of PCM in micron size scale [50]. Based on their preparation method and shell

materials, microcapsules may have different morphologies: (1) mononuclear, which is a single PCM core being covered by a polymeric or inorganic shell; (2) poly-nuclear, which is made of PCM cores of different sizes being dispersed in the shell; and (3) matrix, in which the core material is homogeneously dispersed into the shell [51,52]. Many different polymers have been used to encapsulate various organic and inorganic PCMs. Examples include polystyrene [53], poly(methyl methacrylate-co-divinylbenzene) [54], phenolic resin [55], vinyl trimethoxysilane [56], urea–formaldehyde resin [57], etc. Microencapsulation methods can be subdivided into chemical methods and physical methods. In chemical methods, chemical reactions, such as polymerization, are needed to convert the prepolymer or monomers into an encapsulating shell. In physical methods, there is no chemical reaction and all the ingredients are in their polymeric form during the encapsulation process.

2.3.2.1 Physical encapsulation methods

In this section, two of the most commonly used physical methods for encapsulation of PCM, spray drying and solvent evaporation method, will be discussed. There are some other physical procedures that has been used for encapsulation of different materials. Pan coating is a common method that has been used for encapsulation of pharmaceutical products. In this method, the core and shell materials are mixed together and heated until the shell material is melted and covers all the core material with a higher melting point than the shell. This procedure cannot be used for PCM, since the encapsulating shell must have a higher melting temperature than the PCM. Another physical encapsulation method is air suspension coating. In this method, the core materials are suspended while floating in an air stream. The polymeric solution is sprayed to the floating core particles and covers them, and the particles are then dried. A major disadvantage of

this solution is agglomeration of the final product. No paper has used this method for encapsulation of PCM [50,58].

a) Spray drying

In this method, a feed is converted from a fluid state to a dried solid state after being sprayed to an environment at high temperature. The feed can be a solution, emulsion, suspension or a dispersion. This method consists of four main steps which is shown in Figure 2.1: (1) the atomization of the concentrated feed stock with optimum required condition; (2) evaporation of up to 95% of water content in feed, by means of hot air, which takes place in few seconds in the chamber; (3) spraying the feed and placing the sprayed feed in contact with hot air, until the evaporation is completed; and (4) separating the sprayed particles with cyclone or filter. Agglomerated or uncoated particles are some of the drawbacks of this method [50,59].

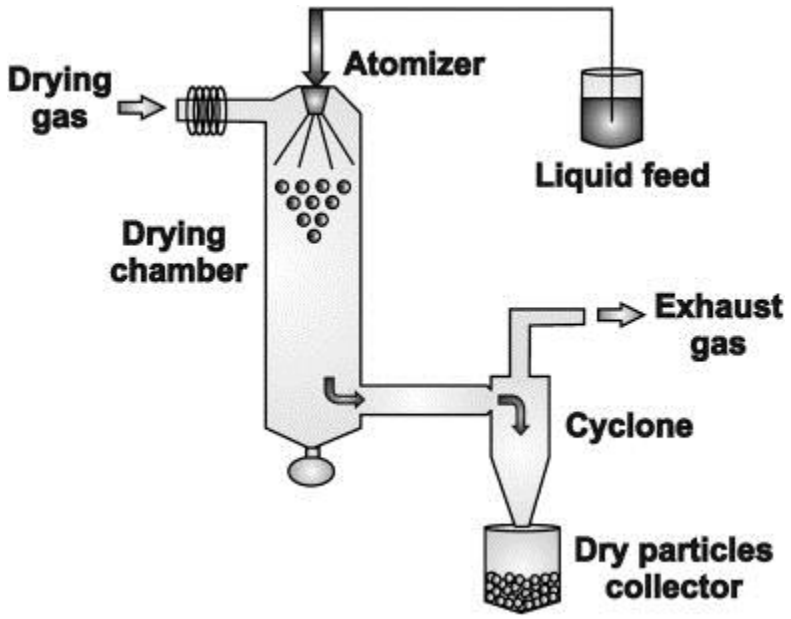

Figure 2.1. The process of spray drying method. Adapted from [60] by permission from the publisher

At the laboratory scale, the yield is about 20-70 %; however, it has a higher yield when used in industrial scale as the percentage of agglomerated or uncoated particles decreases. The ability

of this method in preparing nano-sized particles is limited due to insufficient forces of liquid atomization. Many researchers focus on enhancing the yield and producing nanoparticles by developing better spray dryers [60]. However, this method is widely used in different applications and it is easy to scale up [50]. Hawlader *et al.* [61] encapsulated paraffin wax with gum Arabic and gelatin using spray drying method and got an almost uniform particle size distribution.

b) Solvent evaporation method

Solvent evaporation is widely used for encapsulating different types of medicine and can also be applied to encapsulate PCM. The main advantages of this technique, unlike the polymerization methods, are the high speed and simplicity of the method, no requirement of expensive and toxic chemicals such as initiators, chain extenders, etc., and absence of any residual monomers [62]. Different techniques, depending on the hydrophobicity of the core and shell materials, are required in the solvent evaporation method. The single emulsion method is used for encapsulating hydrophilic materials and the double emulsion methods is a process used for encapsulation of hydrophilic cores. The oil in water (o/w) method, which is used for encapsulating insoluble or poorly soluble core materials in water, is the simplest solvent evaporation method and is a single emulsion technique. This method consists of four basic steps. First, the hydrophobic core material and the polymer to be used for the shell are dissolved in an organic solvent as the oil phase. Then, the oil phase is dispersed by means of agitation energy in a solution containing water and a surfactant. After that, by increasing the temperature or decreasing the pressure, the solvent will evaporate and the polymeric shell covers the cores and solid core-shell particles will be shaped. Finally, the solid particles can be collected by means of filtration or centrifugal force. The particles should be washed for several times with distilled

water or a buffer solution to remove residual surfactants. A schematic of this process is shown in Figure 2.2. Polylactic acid (PLA), poly(lactic-co-glycolic acid) (PLGA) and poly(ethylene glycol) (PLGA) are some of the most common polymers used in this method for pharmaceutical applications [63].

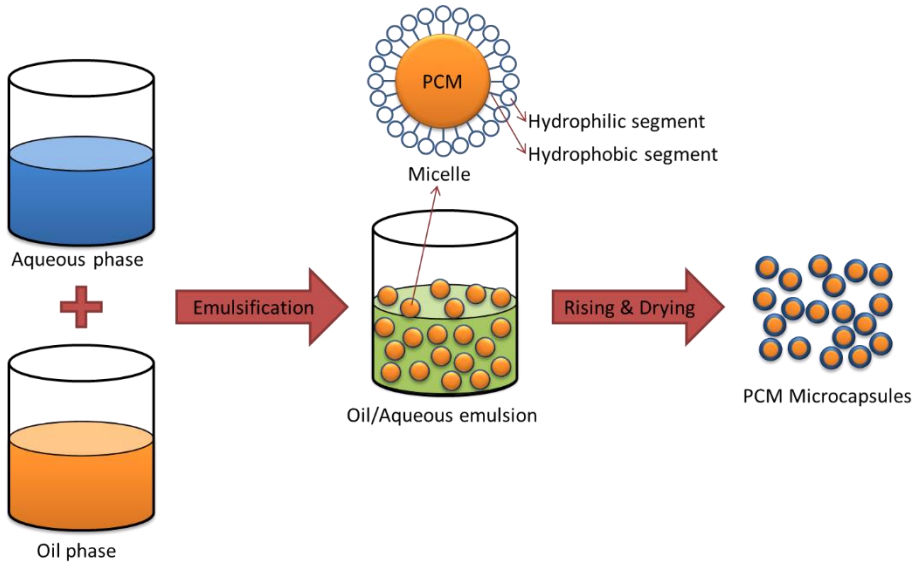

Figure 2.2. Procedures to fabricate 100% bio-based PCM microcapsules

Since organic PCM are typically hydrophobic materials, o/w solvent evaporation is the method used for preparing PCM microcapsules. The size of the microcapsules is influenced by many factors such as: stirring speed, surfactant type and content, viscosity of organic phase and water phase, the ratio of the oil to water phase, temperature, etc. [64]. The organic solvent used in the oil phase must be able to dissolve both the polymer and the core material. Nevertheless, it must not be miscible with water so that a stable emulsion can be formed with the assistance of a surfactant. The should have high vapor pressure and low boiling point to facilitate the evaporation of the solvent at lower temperatures and should be low in toxicity. Dichloromethane (DCM), ethyl acetate and chloroform are some of the most commonly used solvents for this method. DCM has a lower boiling point (39.6°C) than ethyl acetate (77.1°C). Moreover, it is

more hydrophobic than ethyl acetate, which shows partial miscibility in water. Therefore, DCM is the preferred organic solvent to prepare o/w emulsion. However, it is proven that DCM is carcinogenic and its use, especially for pharmaceutical applications, raised some concerns.

However, o/w is not a suitable method for encapsulating hydrophilic core materials such as salt hydrates. First, the hydrophilic core material cannot be dissolved in an organic solvent. Second, it can easily diffuse into the water phase and be removed during the filtration step. Most hydrophilic core materials are encapsulated via the double emulsion (DE) method. There are two common types of double emulsion: water in oil in water (w/o/w) and oil in water in oil (o/w/o), which are prepared in two steps. For making a w/o/w DE, the inner water phase (denoted as W1) is first emulsified in an oil phase with a hydrophobic surfactant. Then, this emulsion is dispersed in a second water phase (denoted as W2) with a hydrophilic surfactant. This method has some disadvantages such as the leakage of the inner water phase into the external aqueous phase, producing non-uniform particles and a more complex process in comparison to the single emulsion method [65].

In addition to the core material, polymeric shell and organic solvent that compose the oil phase, one important ingredient in single or DE methods is surfactant. Surfactants (a mixture of "Surface Active Agents") are amphiphilic materials, which can form micelles and show surface activity. Amphiphilic materials like short chain fatty acids are a class of chemicals which has an affinity for both polar and non-polar materials. One of the most well-known surfactants is detergent. It can change the interfacial properties of a medium and remove the hydrophobic dirt, with the help of water. A typical surfactant has a hydrophilic head and a hydrophobic chain (or tail). The head is responsible for making interactions with the aqueous media with the help of

dipole-dipole forces. In contrast, the tail can make interaction with the organic material. As a result, surfactants can make a connection between hydrophilic and hydrophobic materials [66].

Depending on the nature of the hydrophilic head, surfactants can be sub-divided into four groups with different properties: (1) anionic, which releases a negative charge into the water phase, and has functional groups like sulfate, sulfonate, or carboxylate. The hydrophilic head are usually sodium, potassium, lithium, ammonium, and alkylammonium, especially sodium. The negative anion tail is an active washing component. This group of surfactants are more commonly used globally. Soap, which is a natural product, is the oldest anionic surfactant that has been used for hundreds of years; however, its sensitivity to low pH water and hardness in water, has limited its applications. These flaws have been compensated using synthetic detergents. Anionic surfactants are mostly used in cleaning applications as they are highly functional in removing dirt, clay, and some oily stains. When agitated, they create a higher amount of foam in comparison to other classes of surfactants. (2) cationic, which disperses a positive charge into the water phase, which has functional groups like quaternary ammonium and Cetyltrimethyl ammonium. They usually have chloride and bromide in their structure. They are not common for cleaning products; however, they are mostly used in antistatic agents and antimicrobial cleanser due to its high antistatic and antimicrobial ability. CTAB (Cetyl trimethylammonium bromide) is a cationic surfactant. (3) Nonionic surfactants are the product of a reaction between alcohols, alkylphenols and amines with ethylene oxide and/or propylene oxide. These materials are less sensitive to water hardness and exhibit less foamability. Therefore, they can combine with anionic surfactants and be used in personal care and detergents products. Nonionic surfactants are used as emulsifiers as well. Partially hydrolyzed polyvinyl alcohol (PVA), methylcellulose and Sorbitan ester are some examples of nonionic surfactants;

and (4) amphoteric surfactants that have both anionic and cationic centers on a same molecule. They can enhance the cleaning abilities of cationic and anionic surfactant mixtures. This group is mainly presented by acyl ethylenediamines and alkyl amino acids [67].

Surfactants can reduce the surface tension of the media. The more surfactant added to the water phase, the more surface tension can decrease. However, when the amount of the surfactant reaches the CMC (critical micelle concentration), the surface tension will not change anymore. After reaching the CMC, as shown in Figure 2.3, the micelles are formed [68]. When the surfactant molecules gather together in the shape of a sphere, in a way that the hydrophilic head is outwards and in direct contact with water and hydrophobic tails are incorporated inside, the surface tension is in the lowest possible level [69].

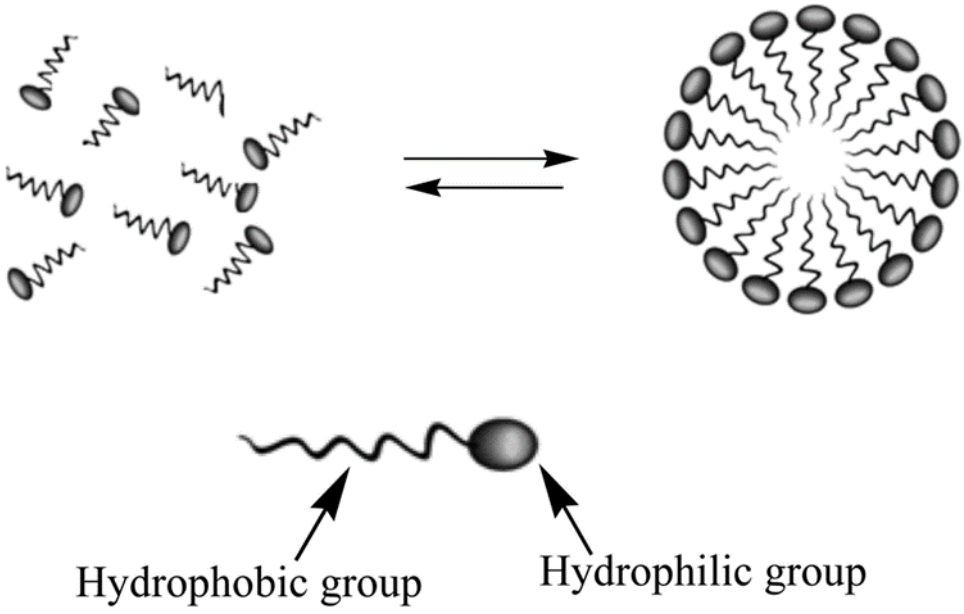

Figure 2.3. Schematic formation of micelles from surfactant particles. Adapted from [70] by permission from the publisher

Surfactants can enhance the dispersion of the oil phase in the water phase, and stabilize the emulsion. This will result in the fabrication of microspheres with smoother surfaces and prevent

agglomeration. Hydrolyzed PVA is one of the mostly used surfactants for the solvent evaporation method [63].

Although solvent evaporation is a widely used method for encapsulating pharmaceutical products, few researchers have used it to encapsulate PCM. Wang *et al*. [71] used the solvent evaporation method to encapsulate paraffin wax by PLA. They used PVA as a surfactant and managed to fabricate particles with average size of 5 to 10 µm. However, the results showed a wide particle size distribution, ranging from 5 to 100 µm. They managed to manufacture particles with a core content of 78%. Core content defines the amount of core material in a microcapsule. This amount is measured using differential scanning calorimetry (DSC). The exact amount of core and shell materials is not mentioned in this report. In almost all previous researches conducted on the PCM, the shell material is a synthetic polymer, which is designed to cover the PCM core by means of chemical methods like different kinds of polymerization. The solvent evaporation method is extensively used to encapsulate different drugs with PLA or PLGA, which are biocompatible and biodegradable polymeric materials. Until now, no one has manufactured a 100% fully bio-based PCM microsphere, and this important aim was fulfilled in this thesis.

To the knowledge of the author, no paper has used the double emulsion method to encapsulate inorganic PCM. However, as mentioned previously, this method has been used in pharmaceutical applications. Like the single emulsion method, bio-based polymers such as PLGA, PLA and poly-(glycolic acid) are commonly used as the drug's polymeric shell. Gaignaux *et al.* [72] used the DE method to encapsulate the clonidine medicine that is used for controlling high blood pressure. They chose PLGA as the encapsulating shell, DCM as the organic solvent, and PVA as the surfactant. The ratio of clonidine to PLGA was 1:100 and in the

final product, the loading was measured to be between 0.2 to 0.49% and the particle size of the microcapsules were 10-30 μm. In another research, Al Haushey *et al.* [73] investigated the effects of different parameters such as agitation time, shell and core materials contents, as well as surfactant content on the encapsulation of bovine serum albumin by polycaprolactone (PCL). They produced particles with high encapsulation efficiency (i.e., 80%), with a smooth surface, and an average particle size of 4 μm. The ratio of core material to polymeric shell was around 0.02. Karal *et al.* [74] prepared protein-PLGA microcapsules with the encapsulation efficiency of 50 to 60 %. They managed to cover 5 μg and 50 μg of protein using double emulsion method.

2.3.2.2 Chemical encapsulation methods

This section reviews three of the most commonly used chemical methods for the preparation of PCM microcapsules. Miniemulsion polymerization, which is based on the suspension polymerization method, is sometimes used for encapsulation of PCM. In this method, the monomers are precipitated in the media and by means of ultrasonic energy, the size of monomer droplets decreases to submicron size (50-500 nm) which is much smaller than monomer particles in suspension polymerization (1-100 μm). The polymerization locus in these two procedures is monomer droplets. Hence the final products in the miniemulsion method is smaller than suspension polymerization [75].

a) Suspension polymerization

Suspension polymerization is a kind of heterogonous radical polymerization that involves two different phases (i.e., aqueous phase and oil phase). As illustrated in Figure 2.4, the aqueous phase usually contains water and a surfactant while the oil phase consists of monomer, initiator (which is soluble in the monomer), PCM (the core material), and sometimes a crosslinking agent. The place in which the monomer dissolves determines the locus of polymerization, which in this

kind of polymerization, takes place in monomer. By means of agitation energy, the oil phase is suspended in the aqueous media and forms droplets in micron size. Different parameters can affect the final size of the particles. These include the oil phase to water phase ratio, stirring speed, the amount of surfactant, and the viscosity of both phases. The average particle size of the product can be predicted by Equation 2.1:

$$\bar{d} = \frac{kD_v R\vartheta_d \varepsilon}{D_s N^2 \vartheta_m C_s} \qquad 2.1$$

where k is a parameter dependent on the type of process; D_v (m) is the diameter of the vessel; D_s (m) shows the diameter of the stirrer; R is the volume fraction of monomer phase; ϑ_d (cP) is the v droplet viscosity; ϑ_m (cP) is the viscosity of the suspension medium and ε (N/m) is interfacial tension between the oil and water phases [50].

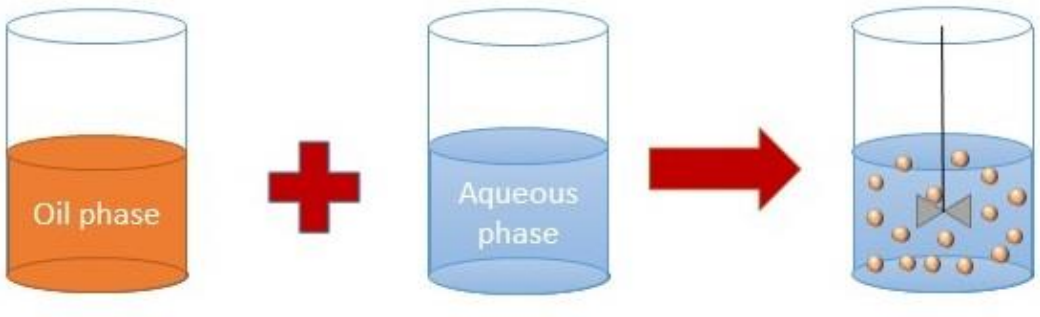

Figure 2.4. Suspension polymerization method used for encapsulation of PCM

After preparing the two-phase system, the initiation of polymerization can be triggered by increasing the temperature to the activation temperature [76]. Poly-(vinyl chloride) and its copolymers, polystyrene, high-impact polystyrene (HIPS), poly(methyl methacrylate) and its

copolymers, as well as poly(vinyl acetate) are some of the commercial polymers produced by this process [77].

Different microPCM have been produced by this method. Sanchez *et al.* [78] produced a comprehensive research on encapsulation of different PCM with this method. They encapsulated commercial grade PRS® paraffin wax, with melting point of 40°C, by suspension copolymerization of styrene (St) and methyl methacrylate (MMA). Experimental results showed that increasing the mass ratio of MMA to St helped speed up the termination of the polymerization and decreased the sizes of the fabricated microPCM. The lowest mass ratio of PCM to monomers that the PCM could be encapsulated was 1/3 and by increasing the amount of PCM, encapsulation remained unsuccessful. The MMA/St ratio had a significant effect on the morphology (spherical and irregular particles) and encapsulation efficiency of the microPCM. The highest core content (43.17%) was obtained in a batch with the MMA/St ratio of 3.5. The cross-section of the microcapsules revealed a poly-nuclear structure. Generally, microPCM prepared by an encapsulation process that involves an emulsification step yields a poly-nuclear structure in the core [79]. By comparing the thermal properties of microPCM with a P-(MMA-co-St) shell with those that have a polystyrene shell, one can understand that including the MMA monomer would enhance the encapsulation efficiency from 20.56 % to 43.17 %. This is caused by MMA's high polarity and reactivity. The hydrophilicity on MMA's structure will help to decrease the surface tension between the oil and water phase and hence helps to have higher core content. In another paper [80], this research group had also shown that two types of polyethylene glycol (PEG), with the molecular weights of 760-840 and 900-1100 $g \cdot mol^{-1}$, could not be encapsulated by polystyrene with suspension polymerization due to its hydrophilic nature. In another paper, Sanchez *et al.* [81] investigated the effect of different surfactants on the

morphology, particle size distribution and thermal properties of the paraffin-polystyrene microPCM. They used polyvinyl alcohol (PVA), polyvinylpyrrolidone (PVP), and arabic gum for their research. Results showed that microPCM fabricated by polyvinylpyrrolidone (PVP) as the surfactant, has a spherical shape and a smooth surface. However, microPCM prepared by polyvinyl alcohol (PVA) and Arabic gum, had an irregular shape and a rough surface. Moreover, when PVA was used as the surfactant, the fabricated MicroPCM had a wide particle size distribution (i.e., 50 μm to 2 mm). This may be due to PVA's high degree of hydrolysis that could not adsorb strongly to the oil/water interface. With a high degree of hydrolysis in PVA, the lypophilic to hydrophilic ratio in this surfactant decreases and its ability to supresse the surface tension reduces. The encapsulation efficiency of microPCM fabricated using PVA was reported to be 55.3 %; however, the reported encapsulation efficiency may not be reliable. While the process yielded a wide particle size distribution, the samples were filtered and only the smallest particles were collected and tested [81].

In another research, Qiu *et al.* [82] investigated the effects of crosslinking agent type (e.g., Divinylbenzene (DVB) and pentaerythritol triacrylate (PETA)) and shell material type (e.g., poly(butyl methacrylate) (PBMA) and poly(butyl acrylate) (PBA)) on the morphology and thermal properties of the fabricated microPCM. Experimental results revealed that using PETA as the crosslinking agent would lead to microPCM with smaller particle size and a narrower particle size distribution. It is believed that the presence of hydrophilic groups in shell materials would promote their compatibility with PETA but not with DVB. However, the microcapsules prepared with DVB showed slightly higher core content (i.e., 55.6% with the PBMA as shell). The samples that were prepared with DVB as crosslinking agents showed higher resistance to elevated temperatures in comparison to the samples prepared with PETA. The authors attributed

this observation to the flexibility of the side chain in BMA and BA. They concluded that introducing a rigid phenyl group of DVB can provide a better mechanical property to the polymeric shell. The improved mechanical property of the shell could enhance the core content in comparison to other conditions. The thermal stability of the samples was tested using heating and cooling cycles and all the samples showed acceptable thermal stability.

b) Emulsion polymerization

Unlike suspension polymerization, the initiator in emulsion polymerization is water soluble. Hence, the locus of the polymerization is no longer the monomer droplets. As stated previously, wherever the initiator is dissolved, the polymerization happens. Under this method, monomers are present in three different regions, which is shown in Figure 2.5. First, large droplets of monomer can be floating in the water phase. Second, small droplets of monomer can be dissolved in the water phase, but this rarely happens due to the hydrophobic nature of the monomer. Third, the monomer droplets can also be present in micelles, in which the monomer molecules are covered by surfactant molecules, and this is the main locus of polymerization in this method. When the concentration of the surfactant molecules reaches a threshold level in the third region (i.e. critical micelle concentration), micelles are formed. Surfactant makes a connection between the oil phase and the water phase. Because of the large surface area of the micelle, the initiator is then adsorbed to it and the polymerization starts in the micelle. Polymerization may also occur in floating monomers; however, due to the small amount of dispersed monomers in the water phase, the polymerized amount in those sites is negligible [83].

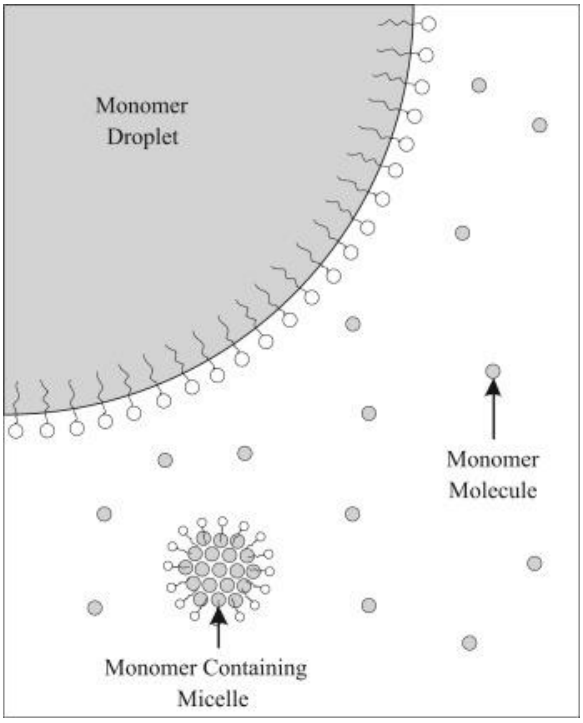

Figure 2.5. Schematic process of emulsion polymerization. Adapted from [50] by permission from the publisher

Sari *et al*. [84] encapsulated a n-nonadecane PCM with poly(methyl methacrylate) (PMMA) shell. Triton X-100 was used as a surfactant and the initiator was an aqueous solution of ferrous sulphate heptahydrate and ammonium persulphate. The thermal reliability of the fabricated microPCM was proven to be great. After undergoing 5000 thermal cycles, the melting point and enthalpy of fusion of the microPCM had negligible variations. The same research group also investigated [85], a eutectic PCM (i.e. capric–stearic acid) as the core and PMMA as the shell material to fabricate microPCM via the emulsion polymerization method. The eutectic's melting point, that was about 31°C, was lower than the individual materials. The highest core content was 65.8 % for the sample with shell-to-core ratio equaled to 2:1. The thermogravimetric analysis (TGA) results revealed that the sample has a good thermal stability up to 80°C, which is higher than the melting point of the PCM.

c) Interfacial polymerization

Similar to the emulsion and suspension polymerization, interfacial polymerization also contains two phases (i.e., water phase and oil phase). The polymerization occurs at the interface of the two phases. Figure 2.6 represents a schematic of interfacial polymerization process. Usually, the water phase contains a diamine, diol, etc. An inorganic base like sodium hydroxide (NaOH), helps activate the diol and naturalize the by-product acid. The oil phase is made of diacid chloride, diisocyanates, etc. and an organic solvent such as hexane, dichloromethane, or toluene. When the two phases are in contact or stirred, the polymer is formed at their interface. In order to encapsulate the PCM using this method, the PCM needs to be dissolved in the oil phase with the help of the organic solvents mentioned above [86,87]. Zhan *et al.* [88] used this method to encapsulate RT21 using isophorone diisocyanate (IPDI) and ethylene diamine (EDA) as monomers to form a polyurea shell. RT21 is a mixture of saturated hydrocarbons, produced by Rubitherm Company with a melting point of 21°C. Hexadecane was the solvent for the oil phase and the influence of different surfactants was investigated on the morphology and thermal properties of the microPCM. The results showed that the micro-particles prepared with Tween60 as a surfactant have a spherical shape and a smooth surface. Tween60 is a brand name and is a mixture of stearic acid and palmitic acid, with a hydrophile-lyophile balance (HLB) of 14.9. Sodium dodecyl benzenesulfonate (SDBS) was another surfactant that was used in this research. Due to the higher HLB of this surfactant (i.e. 21) in comparison to Tween60. The surfactants with high HLB amount are not suitable for preparing oil in water emulsion. This can be caused by the hydrophobicity and good compatibility of Tween60 and polyurea. By increasing the emulsifying stirring speed from 1000 to 4000 rpm, the average particle size decreased from 27.43 to 2.38 μm and the particle size distribution became narrower.

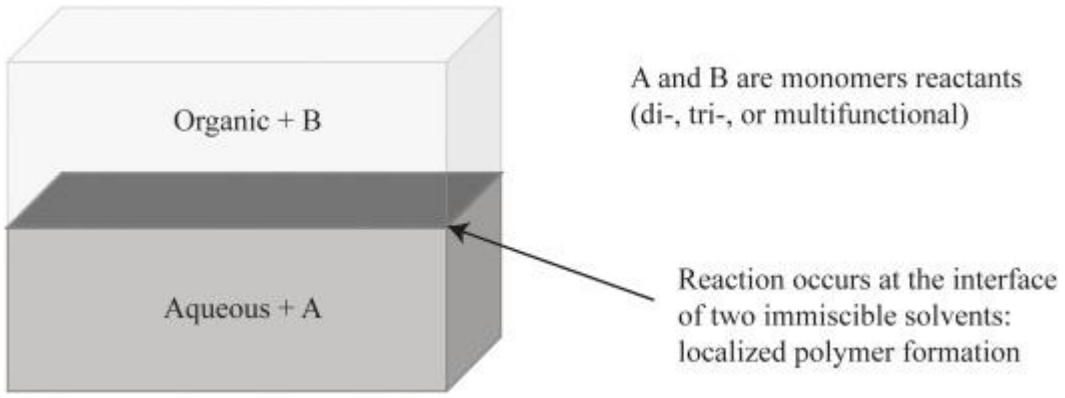

Figure 2.6. Schematic process of interfacial polymerization. Adapted from [89] by permission from the publisher.

2.4. Enhancing the thermal conductivity of PCM

Low thermal conductivity of organic PCM, which is usually in the range of 0.15 to 0.20 W/mK, is their major drawback. To enhance the thermal conductivity of the PCM, different thermally conductive additives have been added to different PCM. Graphite and nano-clays are frequently chosen as fillers to prepare PCM composites because of their low costs and high thermal conductivity. Jeong *et al.* [25] have added bio-based PCM to exfoliate graphite and analyzed the improvement of thermal conductivity and thermal stability of the resultant composites. Yu *et al.* [90] have prepared nanocomposite of 5 wt % bio-based PCM and carbon nanotube (CNT), and observed a 336% increase in the material system's thermal conductivity over pure PCM. Thermal cycling tests have also been applied to the encapsulated PCM or PCM composite to ensure the thermal stability and shell durability. Oya *et al.* [91] investigated the changes in morphology and thermal conductivity of the PCM composites by adding three different kinds of fillers (i.e., spherical graphite, layered graphite, and nickel particles) to erythritol, which has a melting point of 118°C). They added each of the mentioned fillers with a volume ratio of 1-44% (i.e., 1, 2, 3, 6, 7, 8, 14, 15, 24, 34, 44 %) to the molten PCM at 150°C, followed by stirring at 1200 rpm. The liquid composite was transferred to a cylindrical mold and

subsequently dried. Composites filled with expanded graphite exhibited the highest thermal conductivity (i.e., 4.72 W/m·K), even at a volume fraction (i.e., 15%) lower than the composites prepared using the two other fillers. This level of thermal conductivity was 6.4 times higher than the thermal conductivity of pure PCM. In another research, Ji *et al.* [92], manufactured ultrathin graphite foam by chemical vapor deposition. They found that by adding 0.8–1.2 vol.% of this thermally conductive foam to a PCM, the thermal conductivity of the PCM composite system was increased by 18 times. The addition of the graphite foam did not cause any significant change in the melting point or the specific heat of fusion. In all papers mentioned in this section, the filler is directly dispersed in a PCM without any polymeric encapsulation. However, some researchers have dispersed the fillers in polymeric shells and encapsulated the PCM core with this polymeric composite. Chen *et al.* [93] made graphene oxide (GO)-poly(melamine-formaldehyde) microcapsules containing n-dodecanol by in-situ polymerization. They added melamine, formaldehyde and different amounts of GO to an aqueous phase to prepare the pre-polymer solution. The PCM was emulsified in a water phase with the presence of sodium styrene–maleic anhydride copolymer as the surfactant. The pre-polymer solution was then added to the PCM emulsion to initiate the polymerization. By adding 4 wt.% of GO to the PCM microspheres, the thermal conductivity increased by about 66% over that of the pure PCM. The GO-PCM microcapsules showed good thermal stability after 100 thermal cycles.

As a result, based on the requirements of the application that PCM is made for, different types and amounts of fillers can be added to the PCM matrix to enhance the thermal conductivity of this material.

2.5. Applications of PCM

The raised concerns regarding the greenhouse effect and global warming have been on top of any environmental issue in the recent years. About 81% of the greenhouse emission in the USA is caused by carbon dioxide [94]. Also, it is expected that by 2050, the energy demand for buildings will increase by 50% globally [95]. Human activities have major impacts on the emission of CO_2. Burning fossil fuels is one of the major sources of CO_2 emission. As a result, reducing the use of fossil fuels could be a great help in decreasing the emission of CO_2.

In 2013, the global market for PCM was almost 480 million USD and it is predicted that this amount will increase up to 1765 million USD by the year 2020. Europe has been the biggest consumer of the PCM in the world since there are strict regulations to enhance the energy efficiency of the buildings. Europe uses 30% of the world's PCM. In 2013, paraffin waxes were the mostly used type of the PCM worldwide and they had 45% of the global market. Salt hydrates were the second mostly used type with about 33% of the total market [96].

Phase change materials cover a wide range of chemicals and they exhibit different levels of toxicity. Based on the application, a proper PCM should be used to meet the safety requirements. Generally speaking, salt hydrates have different levels of toxicity. They are generally nontoxic; however, they can cause skin or eye irritation. Paraffin waxes can produce toxic fumes when burnt. Vegetable oil are generally nontoxic and environmental friendly. Fatty acids have different levels of toxicity as well. Regarding the eutectics, the toxicity depends on their components [8].

PCM can be installed in active or passive systems for temperature managements in buildings. In a passive system, no mechanical force is applied and the heat is released or absorbed only by means of temperature fluctuations. On the contrary, in the active systems, the thermal release or absorption is caused by an external force, like HVAC (Heating, ventilation, and air conditioning)

systems. Waste heat recovery systems, water heating, greenhouse temperature control systems, frozen food and ice cream preservation and solar cookers are a few other applications of PCM [21,95]. One example of an active system is free cooling. The PCM is installed in a storage unit and placed inside the building. The cold weather of the night is brought to the PCM with the help of the fan and the PCM freezes and passes the energy to the room to keep it warm. During the day, when the temperature of the room has reached beyond the comfort zone, the PCM melts and makes the room cooler [97].

PCM are now used in textiles for enhancing the thermal regulation of different apparel used in cold or hot weather. The encapsulated PCM can be incorporated in the textile, and adsorbs or releases the thermal energy with thermal fluctuations in skin. In another word, the foam, fiber or fabric containing PCM can store the heat created by the body and release it whenever the temperature of the skin is fallen. As a result, the PCM undergoes phase transition for numerous cycles. Up to now, the PCM has been used in different apparel such as space suits for astronauts, sportswear, bedding accessories (i.e. pillows, mattress), shoes, firefighter's suits, automobile seat cover, etc. [98].

PCM can be used for food packaging as well to enhance the temperature protection of the food. The PCM has been embedded in ice cream container to delay the temperature rise of the ice cream when it is placed in room temperature after three hours. The results showed that the temperature of the container covered with 2 cm of PCM was almost 15 degrees cooler than the container without any PCM [99]. The PCM is also sold by the names of cool or warm packs in plastic packages and sold to keep different products like medicine or food cool or warm [100].

In this chapter, different types of PCM and challenges for using them, different encapsulation methods and recent researches regarding this topic were reviewed. For the polymeric shell, it was

shown that synthetic polymers are the most commonly used materials. In contrast, the uses of biodegradable polymers (e.g., PLA) to fabricate the polymeric shell is rare. Also, no paper has reported using bio-derived material like chitin as nucleating agent for inorganic PCM.

Chapter 3
Preparation of 100% Bio-based PCM Microcapsules[1]

MicroPCM represent a unique means to promote substantial energy conservation through their passive thermal regulating and thermal energy storage capabilities. Also, it is possible to promote further their environmental sustainability if both the microscopic shells and PCM cores are bio-based. As a result, the goals of this chapter are to develop a fabrication strategy to produce 100% bio-based microPCM as well as to investigate the effects of different processing parameters on their morphological and thermal properties. In this context, palmitic acid (PA), an organic non-paraffinic PCM with a PLA shell were used herein as case examples of the PCM core and the protective shell, respectively. PA is a fatty acid with negligible supercooling and volume change during phase transition. It also has high latent heat of fusion, superior thermal stability, and no toxicity.

3.1. Experimental

3.1.1. Materials

PLA (Ingeo 8052D NatureWorks LLC) was used as the polymeric shell of the microPCM. PA (Acros organics) was used as the PCM core. 87-89% hydrolyzed polyvinyl alcohol (PVA, Sigma Aldrich) with an average molecular weight of 146000-186,000 $g \cdot mol^{-1}$ and sodium dodecyl sulfate (SDS, Sigma Aldrich, ReagentPlus grade) were used as emulsifiers. Dichloromethane (DCM, Caledon Laboratory Chemical), with the density of 1320 $kg \cdot m^{-3}$, was the organic solvent for the preparation of the oil phase. Deionized water was the aqueous medium. All materials and chemicals were used as received.

[1] Some parts of this chapter has been published in the following paper: M. Fashandi, S.N. Leung, Mater. Renew. Sustain. Energy. 6 (2017) 14.

3.1.2. Preparation of PLA-PA microPCM

Microencapsulation of the PA core in a PLA shell was conducted by the solvent evaporation method accompanied by oil-in-water emulsification [63]. This method has been widely used in the pharmaceutical industry to encapsulate different medicines with bio-based and biodegradable polymers such as PLA and poly(lactic-co-glycolic acid) (PLGA) due to its simplicity and reproducibility [101]. In this method, pre-synthesized PLA is used, and this eliminates the complicated PLA polymerization step. Unlike emulsion polymerization, no monomer, initiator or catalyst is used. Hence, it allows the fabrication of microspheres with high purity [62]. In general, the fabrication process involves four main steps: (1) dissolution of PA and PLA in DCM; (2) emulsification of this organic phase (i.e., dispersed phase), in a continuous aqueous phase of deionized water containing PVA; (3) extraction and evaporation of solvent from the dispersed phase, which transforms the dispersed phase into solid microspheres (i.e., microPCM); and (4) recovery and drying of microPCM to eliminate residual solvent and emulsifier.

For the oil phase, 1.2 g of PLA and different amounts of PA (i.e. 0.4, 0.6, or 0.8 g) were added to DCM. The mixture was stirred for two hours at 36°C, which was lower than the boiling point of DCM (i.e., 40°C), to obtain a uniform PLA-PA solution. For the aqueous phase with PVA as the emulsifier, a uniform PVA solution was prepared by dissolving PVA in deionized (DI) water. The solution was cured for 30 minutes at room temperature to swell PVA. After that, it was heated to 80°C for three hours to ensure complete dissolution of PVA. For the aqueous phase with SDS as the emulsifier, a desired amount of SDS was dissolved in deionized water at room temperature. Subsequently, the oil-in-water emulsion was prepared by adding 5 or 10 g of oil phase solution to 60 g of aqueous solution. The oil-water system was first stirred by a

magnetic stirrer at 200 rpm for three hours at room temperature. The emulsion was then sonicated at an amplitude of 50% level for five minutes using a sonicator probe (QSonica Q700).

Table 3.1. Conditions for the preparation of PLA-PA microPCM

Sample	Oil Phase			Aqueous Phase			Oil-in-Water Ratio
	PLA (g)	PA (g)	DCM (mL)	PVA (g)	SDS (g)	DI Water (g)	
PCM0.4	1.2	0.4	29	5	-	95	1:12
PCM0.6	1.2	0.6	29	5	-	95	1:12
PCM0.8	1.2	0.8	29	5	-	95	1:12
$PCM0.6_{DCM0.5}$	1.2	0.6	14.5	5	-	95	1:12
$PCM0.6_{PVA2}$	1.2	0.6	14.5	2	-	98	1:12
$PCM0.6_{PVA3}$	1.2	0.6	14.5	3	-	97	1:12
$PCM0.6_{PVA4}$	1.2	0.6	14.5	4	-	96	1:12
$PCM0.6_{O/W\times2}$	1.2	0.6	14.5	2	-	98	1:6
$PCM0.6_{PVA2\text{-}SDS2}$	1.2	0.6	14.5	2	2	96	1:12
$PCM0.6_{SDS0.5}$	1.2	0.6	14.5	-	0.5	99.5	1:12
$PCM0.6_{SDS1}$	1.2	0.6	14.5	-	1	99	1:12
$PCM0.6_{SDS2}$	1.2	0.6	14.5	-	2	98	1:12
$PCM0.6_{SDS3}$	1.2	0.6	14.5	-	3	97	1:12
$PCM0.6_{SDS4}$	1.2	0.6	14.5	-	4	96	1:12

In the next step, DCM was evaporated by elevating the emulsion temperature to 70°C while the emulsion was continuously stirred at 200 rpm for one hour. The remaining solution was kept

at room temperature for 48 hours to precipitate the fabricated microPCM. Eventually, microPCM were repeatedly washed with deionized water at 50°C and filtrated to remove the PVA residues. The washed microPCM were dried in a vacuum oven at 50°C for 12 hours. Table 3.1 summarizes the material compositions used to fabricate the PLA-PA microPCM in this work. PCM0.6 was denoted as the base case for comparison purpose.

3.1.3. Characterization of PLA-PA microPCM

The chemical structures of microPCM and each of its components (i.e., PLA and PA) were analyzed using Fourier transform infrared (FTIR) spectroscopy (Bruker Alpha-P FT-IR Spectrophotometer). The spectra were collected by averaging signals from 32 scans at a resolution of 4 cm^{-1} in the range of 400-4000 cm^{-1}. Scanning electron microscopy (SEM) (FEI Company, Quanta 3D FEG) was used to observe the morphologies (i.e., surface features and sphericity) and sizes of microPCM. The fabricated microPCM were sputter coated with gold (Denton Vacuum, Desk V Sputter Coater) before the observation. The particle sizes were obtained by analyzing the SEM micrographs using ImageJ (NIH Image). The interior morphology of microPCM was exposed by microtoming microcapsules using a diamond knife.

The enthalpy of fusion and the melting point of microPCM were determined by a differential scanning calorimetry (DSC) (TA Instrument, DSC Q20). These measurements were performed in the temperature range from 40 to 90 °C at a heating rate of $10°C \cdot min^{-1}$. In order to determine the thermal stability of the microPCM, the enthalpy of fusion was analyzed after samples (i.e., the base case (PCM0.6)) were subjected to 50 thermal cycles at the same temperature range and heating rate.

3.2. Results and Discussion

3.2.1. Chemical Structures of PLA-PA microPCM

The FTIR spectra of PLA, PA, and PLA-PA microPCM (i.e., PCM0.4) are illustrated in Figure 3.1. In this characterization method, infrared radiation is passed through the microPCM samples. Depending on the type of chemical bonds, some of the infrared radiation will transmit while some of it will be absorbed. The resulting spectrum would represent a molecular fingerprint of the sample [102]. From curve (a), it can be observed that PLA had obvious absorption peaks at 2996 and 2946 cm^{-1}, which corresponded to stretching vibration of CH_3 bond in the molecular structure. The sharp peaks around 1747 cm^{-1} and 1180 cm^{-1} are related to the stretching vibrations of C=O and C-O-C bond.

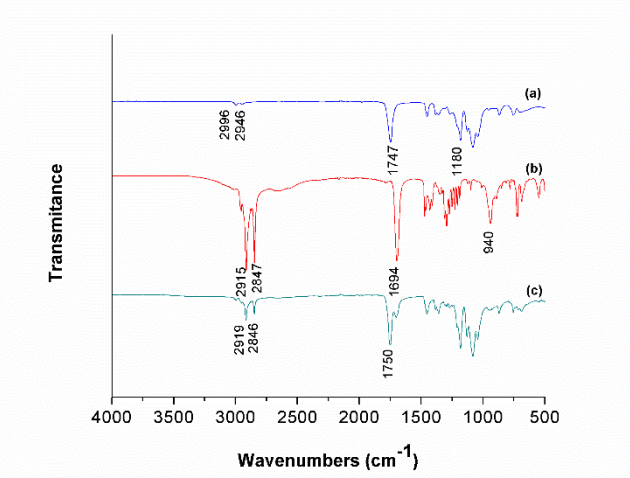

Figure 3.1. FTIR spectra of: (a) PLA; (b) PA; and (c) PLA-PA microcapsules

Curve (b) shows the FTIR spectrum of PA. The sharp peak at 2847 cm^{-1} results from the adsorption by stretching vibration of CH_2 groups and the peak at 2915 cm^{-1} was caused by the stretching vibration of CH_3 group in the PA structure. The absorption band from 2500 cm^{-1} to 3300 cm^{-1} belongs to the stretching vibration of –OH groups and the peaks at 1694 cm^{-1} and

940 cm^{-1} are related to the stretching of C=O and the out of plane bending of –OH, respectively [103,104].

The FTIR spectrum of the PLA-PA microPCM is shown in curve (c). The characteristic peak at 2846 cm^{-1}, attributed to the CH_2 group, belongs to the PA. The absorption peak at 2919 cm^{-1} is related to the CH_3 bond, which were related to both the PLA shell and the PA core. The sharp peak at 1750 cm^{-1} was attributed to the C=O group, which could also be found in both materials. However, the significantly lower transmittance in the peak related to the CH_2 group comparing to the FTIR spectrum of pure PA revealed that both PLA and PA existed in the microPCM. It can be seen that the absorption peaks of PLA-PA microPCM were consistent with those of pure PA and PLA. Therefore, it can be concluded that PA was well encapsulated by PLA resin and no chemical interaction occurred between the core and the shell materials.

3.2.2. Thermal Properties and Thermal Reliability of PLA-PA microPCM

PLA-PA microPCM fabricated using different material compositions were analyzed by DSC to compare their performances and operating temperatures for thermal energy storage. In this method, the differences in the amount of heat required to increase the temperature of the sample and a reference is measured. The sample and reference are kept at a constant temperature during the experiment. If a higher or lower temperature is needed to increase the temperature of the sample, the difference is shown as an exothermic or endothermic process. By observing these differences, the DSC can calculate the amount of required heat for phase transitions and also show the transition temperatures [105]. Pure PA's melting point and latent heat of fusion were 62.8°C and 167.3 J/g, respectively. The latent heat of fusion of microPCM can be determined by integrating the area under the endothermic peak in a DSC thermogram. By comparing this with

the latent heat of fusion of pure PA using Equation 3.1, the core content of PLA-PA microPCM can be calculated.

$$Core\ Content = \frac{\Delta H}{\Delta H_{PCM}} \times 100\% \qquad 3.1$$

where ΔH and ΔH_{PCM} are the latent heat of fusion of microPCM and that of PA, respectively.The melting temperatures, the enthalpies of fusion, and the core contents of different microPCM samples are summarized in Table 3.2. The results show that the melting temperatures for all microPCM samples were virtually unchanged, with a mean temperature and standard deviation of 62.2°C and 0.2°C, respectively. In contrast, the core content was strongly dependent on the PA content as well as the type of emulsifier used. For microPCM prepared using PVA as the emulsifier, as the PA loading increased from 0.4 g to 0.8 g, the core content increased from 24.3% to 41.9%. Nevertheless, changing the DCM content, the PVA content, or the oil-to-water ratio only had minor effects on the core contents of PLA-PA microPCM.

When comparing the two emulsifiers (i.e., PVA and SDS), experimental results reveal that PVA was significantly more effective than SDS for the microencapsulation of PA cores by PLA shells. While all microPCM prepared by using 0.6 g of PA and various amounts of PVA resulted in similar core contents, the endothermic peak of PA was either absent or suppressed in the DSC thermograms of microPCM prepared by using SDS as the lone emulsifier or together with PVA. The hydrophile -lyophile balance (HLB) of SDS is higher than that of PVA [106]. While PVA had a good solubilizing ability to prepare micro-emulsion of oil phase in the aqueous phase, the excessively high HLB value of SDS, together with its high PA solubility, caused it to act as a perfect solubilizing agent to dissolve PA completely in the aqueous phase. As a result, the PA core materials were removed with the aqueous phase in the filtration and washing steps.

Although lowering the SDS content to 1.0 wt.% or below helped to sustain some PA cores in the microPCM, the resultant core contents were significantly lower than those of microPCM prepared using PVA as the emulsifier. As a result, SDS was an inappropriate surfactant for this oil-in-water emulsion system [107].

Table 3.2. Thermal Properties of PLA-PA microPCM

Sample	Melting Point (°C)	Enthalpy of Fusion (J/g)	Core Content (%)
PCM0.4	61.9	40.7	24.3
PCM0.6	62.3	59.9	35.8
PCM0.8	62.1	70.1	41.9
$PCM0.6_{DCM0.5}$	62.4	55.1	32.9
$PCM0.6_{PVA2}$	62.5	52.8	31.5
$PCM0.6_{PVA3}$	62.2	54.3	32.4
$PCM0.6_{PVA4}$	62.3	51.9	31.0
$PCM0.6_{O/W\times2}$	62.0	62.2	37.1
$PCM0.6_{PVA2\text{-}SDS2}$	-	-	-
$PCM0.6_{SDS0.5}$	61.9	33.2	19.8
$PCM0.6_{SDS1}$	62.4	12.0	7.2
$PCM0.6_{SDS2}$	-	-	-
$PCM0.6_{SDS3}$	-	-	-
$PCM0.6_{SDS4}$	-	-	-

The microPCM must maintain their performances in practice after long-term use. Therefore, it is important that they have insignificant change in thermal properties after repeated thermal cycles. In this context, a thermal cycling test was conducted on the microPCM prepared under the base case conditions (i.e., PCM0.6) to determine the thermal reliability of PLA-PA microPCM. After undergoing 50 thermal cycles over a temperature range of 40 to 90°C, the enthalpy of fusion decreased by only 1.0 J/g to 58.9 J/g. This result indicates that there was no chemical degradation in the fabricated microPCM during thermal cycling, and provides evidence to confirm the microPCM were stable chemically after repeated thermal cycling.

3.2.3. Morphology and Size Distribution of PLA-PA microPCM

Figure 3.2 (a) and (b) show the SEM micrographs of a batch of the base case PLA-PA microPCM (i.e., PCM0.6) and the cross-sections of individual microcapsules, respectively. SEM produces the images of the sample by scanning the surface of the sample using electron beam. After the electrons interacted with the sample, they produce signals that has various information about the topography of the sample. SEM can be done in high vacuum or low vacuum conditions [108]. Figure 3.2 (a) reveals that the fabricated microPCM were generally spherical but with a wide range of size distribution and relatively uniform exterior characteristics. This suggests successful microencapsulation of PA cores by PLA shells. The interior features of microPCM were revealed by performing SEM on the microtomed samples. Figure 3.2 (b) illustrates that individual microPCM possessed multi-core morphologies, which was consistent with the general expectation for a microencapsulation process involving an emulsification step [79].

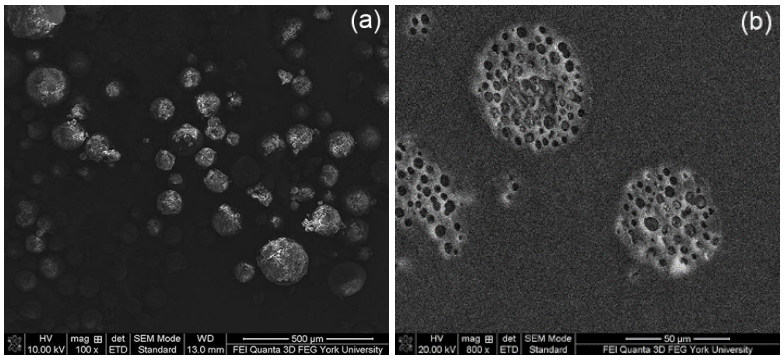

Figure 3.2. SEM micrographs of PLA-PA microPCM (i.e., PCM0.6): (a) a batch of microPCM; and (b) cross-sections of individual microPCM

In this section, the effects of (i) PCM core content; (ii) oil and aqueous media; as well as (iii) emulsifier type and content on microPCM's morphology and size distribution are discussed. The average sizes of microPCM prepared by different material compositions were analyzed using SEM and plotted, with the error bars representing the standard deviations of the microPCM's sizes.

Figure 3.3 plots the average microPCM sizes and the standard deviations for samples consisted of different PA contents. All samples were fabricated at the same processing conditions as the base case. The results reveal that increasing PA contents would slightly increase microPCM's average sizes as well as the degrees of size variation. Research related to the encapsulation of drug by the solvent evaporation approach reported that increasing the viscosity of the dispersed phase in the emulsion would increase the size of the microcapsule. This relationship was expressed as an empirical model in Equation 3.2 [63]. When preparing PLA-PA microPCM, increasing the PA content would increase the viscosity of the dispersed phase, and thereby resulted in larger microPCM sizes.

$$d = A\left(\frac{\mu_d}{\mu_c}\right)^{0.25} \times 100\% \qquad 3.2$$

where d is the average diameter of the microspheres, A is a coefficient dependent on process conditions, μ_d is the viscosity of the dispersed (oil) phase and μ_c is the viscosity of the continuous (aqueous) phase.

Figure 3.4 (a) through (c) shows SEM micrographs of microPCM consisting of 0.4, 0.6, and 0.8 g of PA while keeping a fixed PLA content (i.e., 1.2 g). It can be observed that the microPCM's shapes and surface morphologies were virtually unchanged as the PA content increased. Furthermore, while the microPCM demonstrated their sphericity, some uneven surface morphologies with the presence of tiny microspheres were observed.

The effects of oil and aqueous media on the microPCM morphologies and sizes were investigated by varying either the amount of DCM or the oil phase-to-aqueous phase ratio. Figure 3.5 reveals that the average size of microPCM decreased as the oil phase-to-water phase ratio is doubled. This can be attributed to the reduced amount of emulsifier (i.e., PVA) in the emulsion system, which enhances the ability for the PVA molecules to adsorb on the surface of the dispersed oil phase instead of forming PVA micelles. The governing mechanism of this observation can be found in the later part of this manuscript when discussing the effects of emulsifier content on the microPCM's sizes and morphologies. Figure 3.6 (a) shows the SEM micrograph of microPCM prepared by using half the DCM volume of the base case when preparing the oil phase.

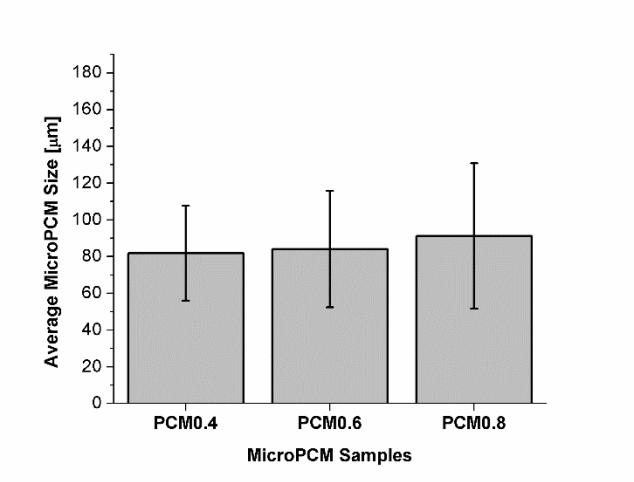

Figure 3.3. Effect of PA content on microPCM's sizes

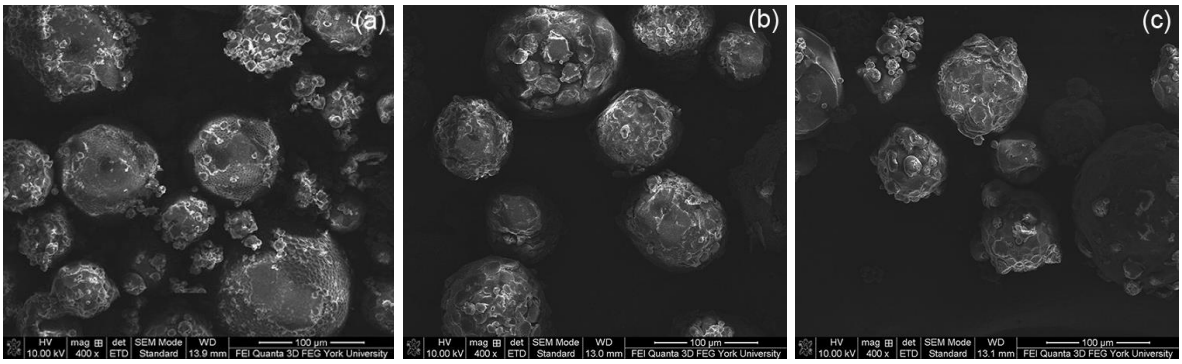

Figure 3.4. SEM micrographs of PLA-PA microPCM consisting of different core contents: (a) PCM0.4; (b) PCM0.6; and (c) PCM0.8.

It can be observed that reducing the DCM content resulted in a higher degree of microPCM agglomerations as well as rougher surfaces. Reducing the amount of organic solvent used would increase the viscosity of the dispersed phase, and thereby led to larger microPCM sizes as shown in Figure 3.6. This trend was again consistent with the prediction based on Equation 3.2 . By comparing Figure 3.6 (b) to Figure 3.4 (b), it can be observed that the sphericity and surface morphology of microPCM were not affected by changing the oil phase-to-aqueous phase ratio from 1:12 to 1:6 in the emulsion.

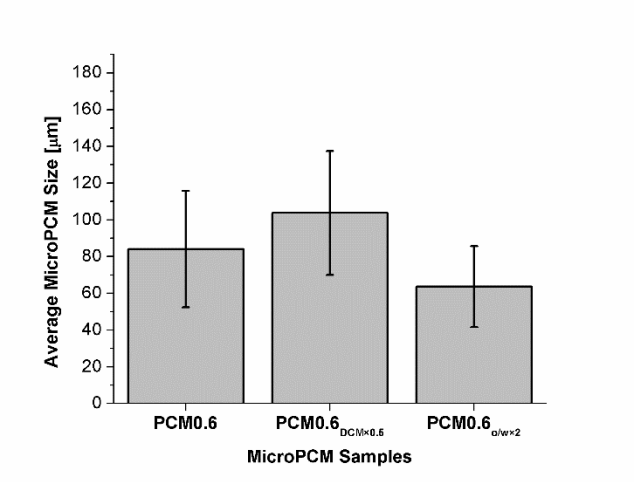

Figure 3.5. Effects of oil and aqueous media on microPCM's sizes

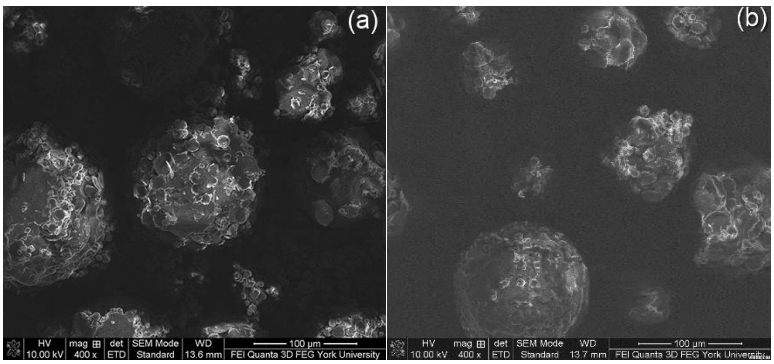

Figure 3.6. SEM micrographs of PLA-PA microPCM fabricated by different material compositions: (a) PCM0.6DCM×0.5 and (b) PCM0.6O/W×2.

Different loadings of two different emulsifiers (i.e., SDS and PVA) were used to prepare microPCM. Comparing the two types of emulsifier, as shown in Figure 3.7 and Figure 3.8, the uses of SDS eased the filtration and washing steps during the fabrication process. Unlike the case of using PVA as the emulsifier, no residues of surfactant were seen in the samples prepared by SDS. It is believed that this can be attributed to SDS's higher HLB and its higher solubility in water.

The effects of emulsifier contents on the microPCM's surface morphologies and sizes were studied. Figure 3.7 (a) and (b) show that, regardless of the type of emulsifier, there existed a U-

shaped relationship between the emulsifier content and the average microPCM size. By increasing the amount of emulsifier from a very low content, more surfactant molecules were available to adsorb to the oil-water interface and reduce the surface energy. This would allow the dispersed oil phase to achieve smaller droplet sizes, which also yielded larger total surface area. However, when the emulsifier content continued to increase beyond a threshold concentration, the fabricated microPCM became larger. This threshold concentration is called the critical micelle concentration (CMC) in the oil-in-water emulsion. Over the CMC, excess PVA molecules would more likely form micelles among themselves, rather than adsorbed on the surfaces of the dispersed oil phase [109,110]. This reduced affinity of the surfactant molecules at the oil-water interfaces would promote the aggregation of dispersed oil phase, and thereby led to the formation of larger microPCM. This was evidenced by the presence of small microspheres (i.e., PVA micelles) on the surfaces of microPCM, as shown in Figure 3.4 (a) through (c), in all samples prepared by using 5 wt.% of PVA solution as the aqueous phase. In contrast, the PVA residues were virtually invisible on the surfaces of the microcapsules and there were negligible agglomerates in Figure 3.4 (b) and Figure 3.6 (a). This could be attributed to the lower number PVA molecules caused by the reduced concentration of PVA or decreased amount of aqueous phase. Furthermore, it is also interesting to note that, for microPCM prepared using SDS, reducing the emulsifier content to 0.5 wt.% would yield very small number of microPCM while a large amount of un-encapsulated materials were observed. In other words, the extremely low emulsifier content caused a low encapsulation efficiency of the PA core. As discussed in the section 3.2.2, this low SDS content was investigated in attempt to overcome the loss of PA to the aqueous phase when higher loading of SDS was used.

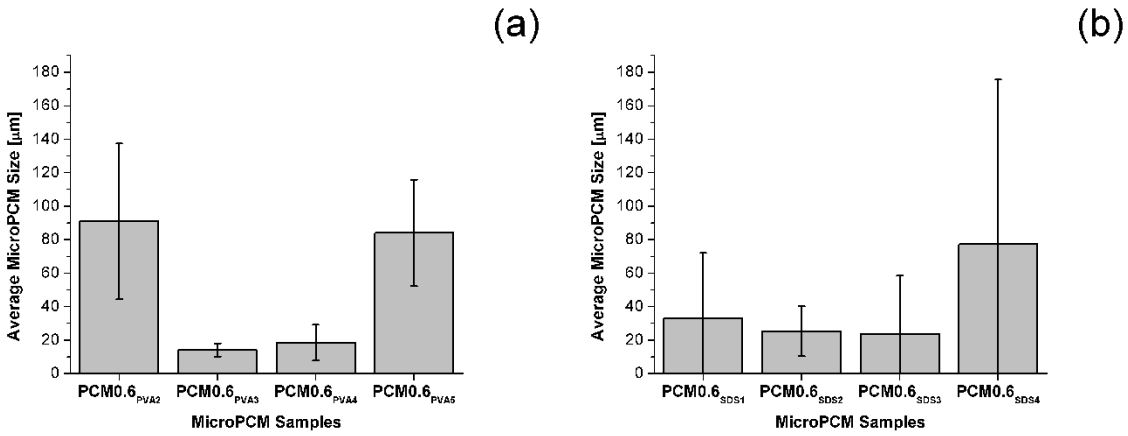

Figure 3.7. Effects of emulsifier type and content on microPCM's sizes: (a) PVA and (b) SDS

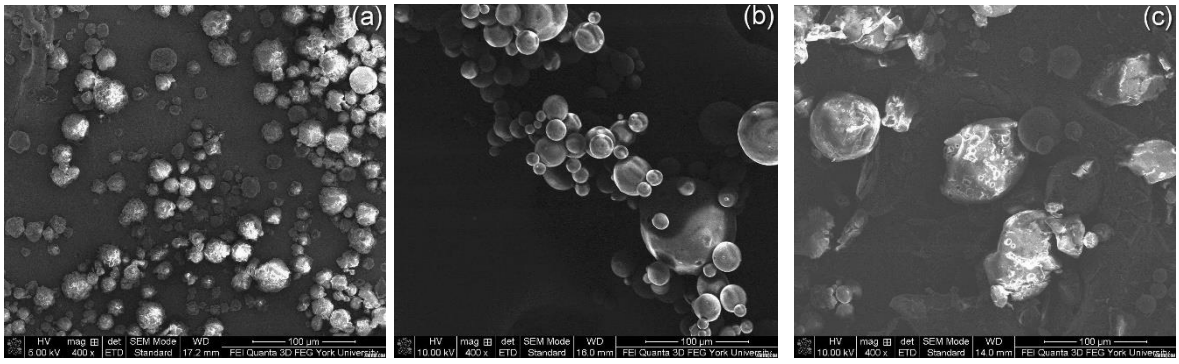

Figure 3.8. SEM micrographs of PLA-PA microPCM fabricated by different material compositions: (a) PCM0.6PVA3; (b) PCM0.6SDS3; and (c) PCM0.6SDS0.5

3.3. Conclusion

Solvent evaporation method, which is commonly used in the pharmaceutical industry for drug encapsulation, was applied to microencapsulate a bio-based PCM [i.e., palmitic acid (PA)] with a bio-based polymeric shell [i.e., polylactic acid (PLA)]. Successful encapsulation of PA core by PLA shell was confirmed by Fourier transform infrared analyses. Parametric studies were conducted to investigate the effects of core content, organic solvent content, emulsifier type and content, as well as oil phase-to-aqueous phase ratio on the characteristics of PLA–PA microPCM. Experimental data indicated that higher PA content yields higher core content.

Moreover, increasing the PA content or decreasing the DCM content slightly increases the microPCM's size due to the higher viscosity of the oil phase.

Regardless of the type of emulsifier (i.e., PVA and SDS), increasing the emulsifier content below the critical micelles concentration (CMC) would reduce the microPCM size due to the reduction of surface energy at the oil-to-water interface by the surfactant. However, further increase in emulsifier content above this threshold concentration would result in larger microPCM sizes. This can be attributed to the tendency of PVA molecules to form micelles among themselves. Furthermore, while the high hydrophile-lipophile balance of SDS led to smoother microPCM surfaces, its high solubilizing capability also led to the dissolution of PA in the aqueous phase. This resulted in the loss of PA and very poor encapsulation efficiency. Therefore, SDS was not a proper surfactant for PA-PLA microcapsules. In short, successful fabrication of 100% bio-based microPCM is expected to promote further the environmental sustainability of the already environmentally friendly latent heat energy storage technology.

Chapter 4
Tuning the Thermal Properties of Inorganic PCM and Preparation of Inorganic PCM Microcapsules

Inorganic PCM show promising properties such as higher latent heat of fusion, higher thermal conductivity, and lower cost than organic PCM. However, supercooling and phase segregation are two main disadvantages of salt hydrates, a main subcategory of inorganic PCM. Adding an external nucleating agent and increasing the viscosity of the salt hydrate using a thickening agent, are two main strategies to prevent supercooling and phase segregation, respectively. Sodium acetate trihydrate (SAT) is an inorganic salt hydrate that is non-toxic, inexpensive, widely available, and thereby has a high potential for thermal energy storage. With its suitable melting point (i.e.58°C) and high latent heat of fusion 258 $J \cdot g^{-1}$, SAT can be a good candidate to be used in solar heating systems. This chapter investigated the possibility of using a bio-based nanoparticle, chitin nanowhisker (CNW), as a nucleating agent to suppress the supercooling of SAT. In an effort to enhance the phase change performance of SAT, a series of parametric studies were conducted to enhance the thermal behavior, thermal stability and thermal conductivity of SAT. Also, a series of experiments were conducted to investigate the possibility of encapsulating SAT with a PLA shell the using solvent evaporation method.

4.1. Experimental

4.1.1. Materials

Sodium acetate trihydrate (SAT, BioXtra, purity >99%, Sigma Aldrich) was used as the inorganic PCM. Sodium carboxymethyl cellulose (CMC, average molecular weight of 250,000, Sigma Aldrich) and sodium dodecyl sulfate (SDS, ReagentPlus, purity >98.5%, Sigma Aldrich) were selected as the thickening agent and the surfactant, respectively. Chitin nanowhisker (CNW, BOCO Technology Inc.), with its physical properties shown in Table 0.1, was the nucleating agent being investigated in this work. Hexagonal boron nitride (hBN, AC6041, Momentive Performance Materials) and graphene nanoplatelets (GNP, CheapTubes Inc., Grade 2), were the thermally conductive fillers used to promote the heat transfer property of the SAT-CNW nanocomposites. The mean lateral size and thickness of hBN were 6 μm and 0.5 μm, respectively. The mean lateral size and thickness of GNP were 25 μm and 10 nm, respectively. All materials and chemicals were used as received.

Table 0.1. Physical properties of chitin nanowhisker (CNW)

Property	Value	Unit
Density	1450	$kg \cdot m^{-3}$
Length	200-500	nm
Width	10-20	nm
Specific Surface Area	72	$m^2 \cdot g^{-1}$

4.1.2. Preparation of the SAT-CNW nanocomposites

PCM nanocomposites consisting of SAT, CNW, and other additives (i.e., CMC, SDS, and/or thermally conductive filler) were prepared mechanically by dry blending. In the first step, SAT

chunks were ground into fine powders by a mill freezer (SPEX SamplePrep Group, model 6770, Freezer/Mill). The fine SAT powders were then divided into various sizes by a stack of sieves with different mesh sizes. 3 wt.% of CMC and various loadings of SDS were subsequently added to the sieved SAT powders of a specific size range. This was followed by the addition of different contents of CNW into the mixture. In order to investigate the effects of hBN and GNP on the effective thermal conductivity of SAT-CNW nanocomposites, different amounts of these thermally conductive fillers were added. Finally, the materials were mechanically mixed using a mortar and pestle before being loaded into a test tube sealed by a rubber stopper. Key parameters being investigated in this work are summarized in Table 0.2. It must be noted that the base case of SAT-CNW nanocomposite consists of 1.0 wt.% of CNW, 0.25 wt.% of SDS, and 3 wt.% of CMC. In the base case, the SAT particle size was smaller than 53 μm. Moreover, no thermally conductive filler was added, and the initial heating temperature was set at 70°C. The effect of each parameter was investigated by varying the specific parameter while fixing the others.

Table 0.2. Key parameters being investigated in this work

Property	Value	Unit
CNW Content	0.6, 0.8, 1.0, 1.2	wt.%
SAT Particle Size	<53, 53-250, 250-500, >500	μm
SDS Content	0, 0.25, 0.50	wt.%
Heating Temperature	65, 70, 75	ºC
hBN/ GNP Content	1, 3, 5	wt.%

4.1.3. Characterization of the SAT-CNW nanocomposites

Three test tubes loaded with 5.0 g of SAT-CNW nanocomposites of the same composition

were heated in a temperature-regulated water bath at a preset heating temperature. A thermocouple, with its tip located at the center of each sample, was connected to a data acquisition system to record the sample's temperature at a sampling rate of 1 Hz. After completely melting the samples, the test tubes were removed from the hot water bath and left in air at ambient temperature for cooling the samples to room temperature. The temperature versus time graphs were then plotted to analyze the cooling behavior and the supercooling degree of each sample. Differential scanning calorimetry (DSC, TA Instrument, Q20) was used to measure the latent heat of fusion and melting temperature of each sample. Thermal analyzes were performed in a temperature range of 40ºC to 70ºC at a heating rate of $10^{o}C \cdot min^{-1}$. The effective thermal conductivity of SAT-CNW nanocomposites was measured by a thermal conductivity analyzer (C-Therm Technologies Ltd., TCi™ Thermal Conductivity Analyzer).

4.2. Results and discussion

4.2.1. The effect of CNW content on the supercooling of SAT-CNW nanocomposites

SAT-CNW nanocomposites containing different loadings of CNW (i.e., 0.6 wt.% to 1.2 wt.%) as the nucleating agent were prepared. One set of samples, without adding CNW, were also made as control. The freezing behaviors of various samples after their first melting at 70°C were recorded. Figure 4.1(a) and 4.1 (b) plot the cooling curves of different samples and their average supercooling degrees with the corresponding standard deviations, respectively. It can be observed that pure SAT suffered from significant supercooling and did not freeze even after it had been cooled down to ambient temperatures. By adding CNW as the nucleating agent and gradually increased the its loadings from 0.6 wt.% to 1.2 wt.%, the degrees of supercooling of SAT-CNW nanocomposites decreased from approximately 10°C at 0.6 wt.% loading of CNW to a minimum of below 0.9°C at 1.0 wt.% loading of CNW. However, when the CNW loading

further increased to 1.2 wt.%, the supercooling degree increased to approximately 14.5°C. These results revealed the high potential of using CNW as an epitaxial nucleating agent to suppress the supercooling of SAT. It is believed that the similar specific densities of CNW and SAT prevented the bio-derived nanoparticles from sediment. The hydroxyl (OH) functional group on CNW also promoted their compatibility with SAT. Together with the increased melt viscosity attributed to the addition of CMC, it resulted in satisfactory dispersion of CNW when its loading was at or below the optimal level. Therefore, increasing CNW loading resulted in an increased number of heterogeneous nucleating sites, and thereby reduced the nanocomposites' supercooling degrees. Nevertheless, when the loading of CNW further increased to 1.2 wt.%, the bio-derived nanoparticles became more likely to aggregate due to their extremely high specific surface areas. In other words, the number density of nucleating sites would reduce, and thereby deteriorate the effectiveness of CNW as nucleating agents to suppress supercooling.

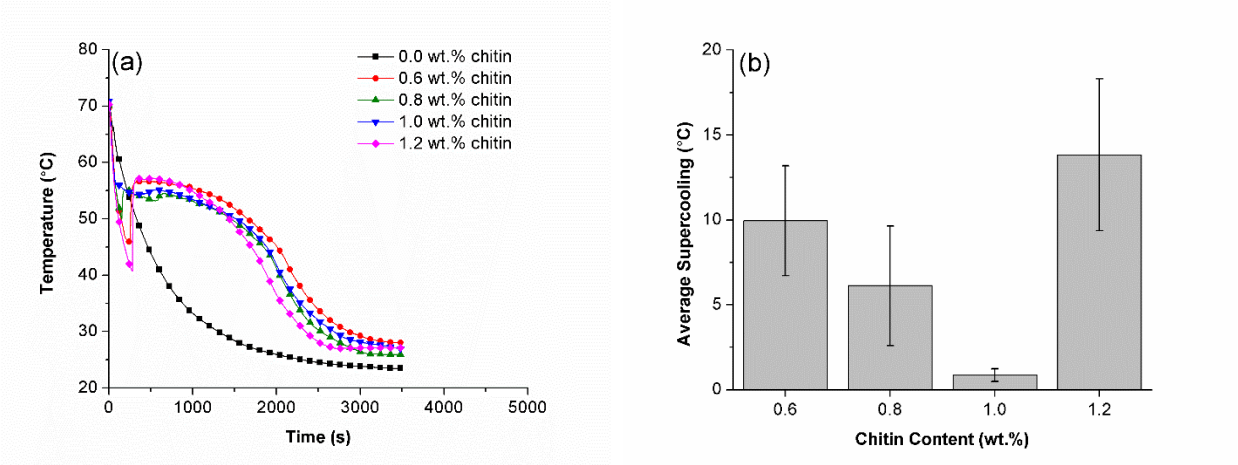

Figure 0.1. The freezing behaviors of SAT-CNW nanocomposites with different chitin contents: (a) Cooling curves; and (b) supercooling degrees

4.2.2. The effect of heating temperature on supercooling degrees of SAT-CNW nanocomposites

The effect of heating temperature (i.e., the temperature of the water bath) on the supercooling degrees of SAT-CNW nanocomposites was studied by varying the heating temperature of the base case sample from 65°C to 75°C. The cooling curves were plotted in Figure 0.2(a) and the observed supercooling degrees are illustrated in Figure 0.2(b). It can be observed that the supercooling degrees of SAT-CNW nanocomposites remained almost constant when the heating temperature increased from 65°C to 70°C. However, further raising the heating temperature to 75°C drastically increased the supercooling degree of the SAT-CNW nanocomposite from 0.87°C to over 30°C. Therefore, it can be concluded that the heating temperature of the energy storage phase during operation would directly influence the supercooling degrees of SAT-CNW nanocomposites. Literature reported that the dehydration of pure SAT can occur when the heating temperature is higher than 30°C [111]. Despite the addition of CMC as a thickening agent to circumvent the problem of phase segregation, excessive increase in the heating temperature (i.e., 75°C) would likely lead to loss of water content from SAT. This would as a result attenuate its nucleation ability. Therefore, although higher heating temperature would shorten the melting cycle, it is critical to ensure the heating temperature does not exceed the operating limit of SAT-CNW nanocomposites in thermal energy storage applications.

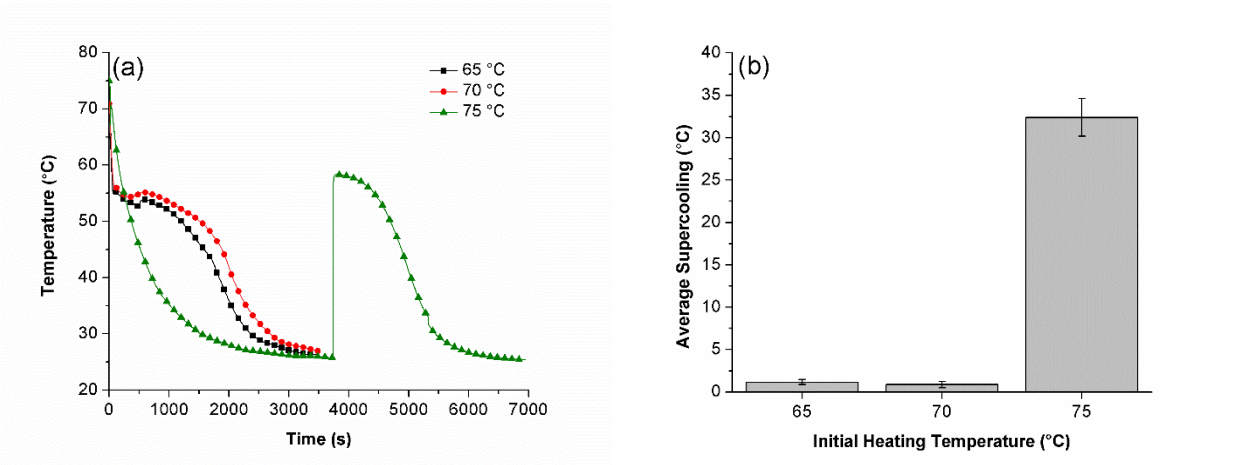

Figure 0.2. The freezing behaviors of SAT-CN nanocomposites at different initial heating temperatures: (a) Cooling curves; and (b) supercooling degrees

4.2.3. The effect of SAT particle size on the supercooling of SAT-CNW nanocomposites

The SAT particle size would likely affect the uniformity of CNW nanoparticles in the mixtures prepared by dry blending. To investigate this, sieved SAT powders of four size levels: (i) < 53 μm, (ii) 53 μm – 250 μm, (iii) 250 μm – 500 μm, and (iv) > 500 μm were used to prepare the samples. The cooling curves and the supercooling degrees are plotted in Figure 0.3(a) and Figure 0.3(b), respectively. Experimental results indicate that increasing the particle size of SAT was detrimental to the supercooling degrees of the SAT-CNW nanocomposites. The particle size plays an important role in the blend homogeneity of the mixture and its effect can sometimes be even higher than the density of each component. When the SAT particle sizes were large, segregation of CNW nanoparticles might occur due to sifting effect [112]. This could be attributed to a higher chance of sifting of the smaller particles to the bottom through the larger interstitial sites among the SAT particles during the initial mixing stage. In contrast, by reducing the particle size of SAT, a better mixing could be obtained due to the smaller particle size distribution of all components in the sample. This led to a more uniform dispersion of nucleating agents in the nanocomposites, and thereby a higher degree of suppression of supercooling. Even

though the SAT matrix melted during the heating cycle, the high viscosity of the melt attributed to the addition of CMC would restrict the translational movement of CNW nanoparticles. In other words, the initial homogeneity of the dry mixture still played a significant role in the phase change performance of the nanocomposites.

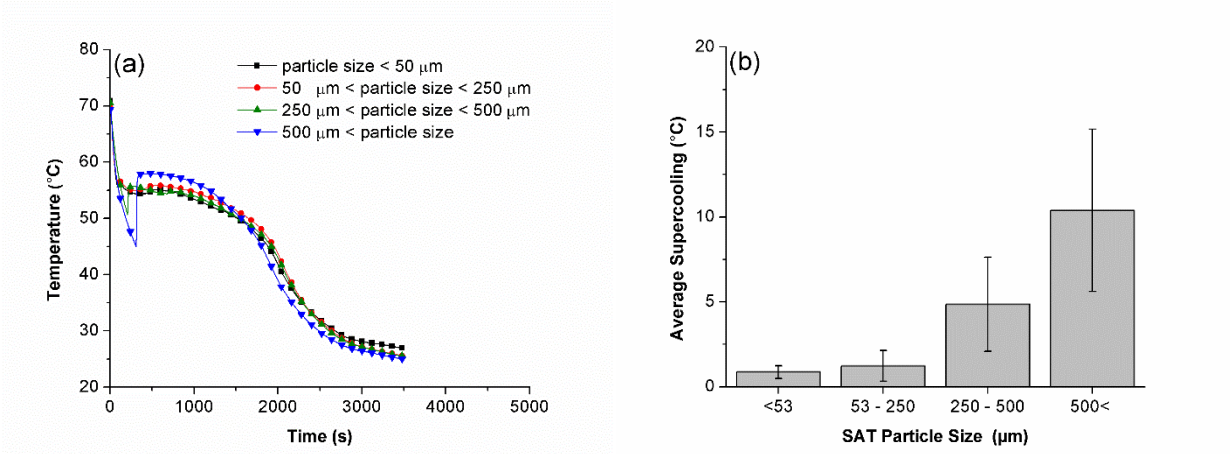

Figure 0.3. The freezing behaviors of SAT-CNW nanocomposites with different SAT particle sizes: (a) Cooling curves; and (b) supercooling degrees

4.2.4. The effect of surfactant content on the supercooling of SAT-CNW nanocomposites

The effect of surfactant content on the supercooling of SAT-CNW nanocomposites was investigated by varying the amount of SDS from 0.0 wt.% to 0.5 wt.% and observing their freezing behaviors after melting them at 70°C. Figure 0.4(a) and Figure 0.4(b) show the cooling curves and supercooling degrees of SAT-CNW nanocomposties loaded with different SDS contents.

Experimental results revealed that the addition of SDS was crucial to prevent the supercooling of SAT-CNW nanocomposites. By adding 0.25 wt.% SDS to the nanocomposite, the supercooling degree dropped from 16°C to 0.87°C. It is believed the addition of SDS enhanced and sustained the uniform dispersion of CNW in the SAT matrix. Further increase in surfactant content to 0.50 wt.% had negligible effect on the supercooling degree of the SAT-

CNW nanocomposite. This demonstrated that adding a small amount (i.e., 0.25 wt.%) of SDS was sufficient to ensure good nucleating agent dispersion throughout the SAT matrix.

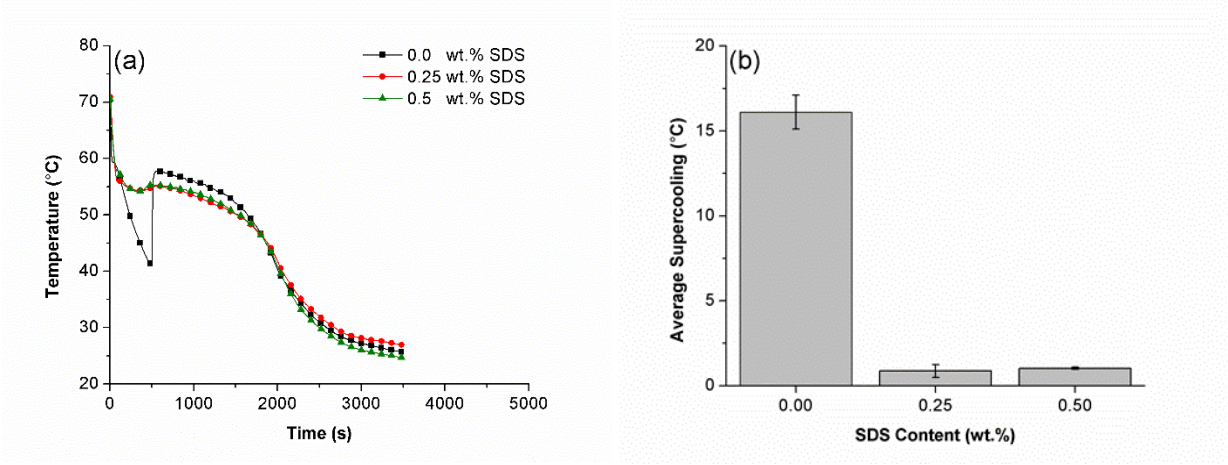

Figure 0.4. The freezing behaviors of SAT-CNW nanocomposites with different SDS contents: (a) Cooling curve; and (b) supercooling degrees

4.2.5. The effects of filler type and content on the supercooling and the effective thermal conductivity of SAT-CNW nanocomposites

While it has been demonstrated that CNW is an effective nucleating agent to suppress the supercooling degree of SAT, high performance PCM should also have high thermal conductivity to facilitate heat transfer. In light of this, the effects of two thermally conductive fillers (i.e., hBN and GNP) on the effective thermal conductivity of the SAT-CNW nanocomposites were investigated. The in-plane thermal conductivity of hBN and GNP are 300 W/m·K and 3000 W/m·K, respectively. hBN has a similar layered molecular structure as graphite and is sometimes called “white graphite”, while GNP consists of several sheets of graphene. Several control experimental trials had been conducted by preparing SAT-hBN and SAT-GNP composites without CNW to investigate the nucleating power of hBN or GNP. Experimental results revealed that neither hBN nor GNP was effective to suppress supercooling as the melted composites did

not crystalize when the samples' temperatures dropped to ambient condition. Thus, their main function was primarily to enhance the effective thermal conductivity of the nanocomposites.

Effective thermal conductivity measurements were conducted to evaluate the effects of different loadings of hBN and GNP on the heat transfer abilities of SAT-CNW nanocomposites. For each composition, three disks with thicknesses of 3 mm and diameters of 10 mm were prepared using a compression molding machine and the measurements for nanocomposites filled with hBN and GNP are plotted in Figure 0.5(a) and Figure 0.5(b), respectively. The thermal conductivity analyzer has a spiral heating element and a known current is applied to it to generate a small amount of heat. The sensor is designed in a way that it only provides one dimensional heat to the sample. The applied current increases temperature the heat at the sample/ sensor interface and the voltage drop is changed in the sensor. This change in the voltage determines the thermal properties of the sample. The results showed that the pure SAT sample's thermal conductivity was 0.70 $W \cdot m^{-1}k^{-1}$. By adding 1 wt.% of CNW as the nucleating agent, the effective thermal conductivity raised to 0.74 $W \cdot m^{-1}k^{-1}$. This negligible change revealed that CNW was not an effective filler to enhance SAT's heat transfer ability. Furthermore, by adding 1 wt.% of hBN and GNP to the SAT-CNW nanocomposites, the effective thermal conductivity increased from 0.74 $W \cdot m^{-1}k^{-1}$ to 0.98 $W \cdot m^{-1}k^{-1}$ for both fillers.

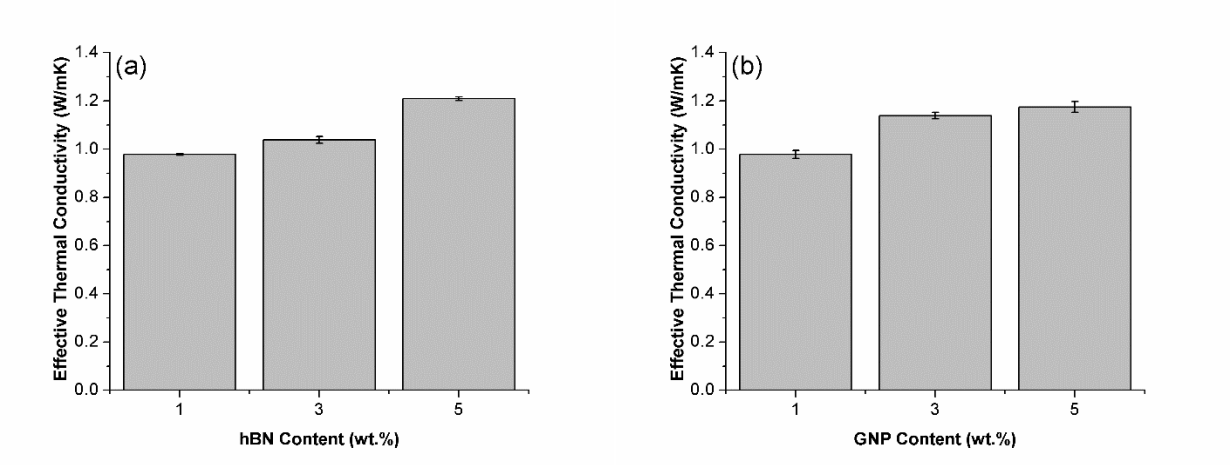

Figure 0.5. Effects of hBN and GNP contents on the effective thermal conductivity of SAT-CNW nanocomposites

By further increasing the hBN and GNP contents to 3 wt.% and 5 wt.%, the nanocomposites' effective thermal conductivity could reach as high as 1.2 $W \cdot m^{-1}k^{-1}$. The results confirm both hBN and GNP were effective to enhance the heat transfer abilities of SAT-CNW nanocomposites. It should be noted that although the pure GNP has a higher thermal conductivity than hBN, the amount of enhancement in thermal conductivity of SAT- hBN and SAT-GNP were the same. The reason lies behind the compatibility of SAT and GNP. If the matrix and filler have weak contact at their interfaces, interfacial thermal resistance would increase and the resultant effective thermal conductivity would decrease [113]. In the beginning of this section, it was explained that the chemical compatibility of GNP with SAT is less than that of SAT with hBN. Therefore, although GNP is more thermally conductive than hBN, the effective thermal conductivity enhancement by them were similar. The cooling curves and the degrees of supercooling of SAT-CNW nanocomposites loaded with different contents of hBN or GNP are shown in Figure 0.6 and Figure 0.7. Experimental results revealed that adding 1 wt.% of hBN to the base case composition slightly decreased its average supercooling degree to 0.62°C. It is believed that the presence of amino groups (NH_2) and hydroxyl groups (OH) on the edge planes of hBN platelets [114] would promote their compatibility with SAT as well as CNW. The

resultant homogeneous dispersion of hBN would be beneficial to SAT crystal nucleation. However, Figure 0.6(a) and Figure 0.6(b) show that further increase in hBN content to 3 wt.% and 5 wt.% increased the supercooling degrees of SAT-CNW nanocomposites to 4.00°C and 5.83°C, respectively. The presence of the highly polar functional groups was limited on the edge planes of hBN. Therefore, excess amounts of hBN platelets would likely form agglomerates and disturb the interaction between CNW and SAT. This led to the undesired increase in SAT-CNW nanocomposite's supercooling despite the promotion in their heat transfer properties. In Figure 0.7(a) and Figure 0.7(b), it can be observed that the addition of GNP, regardless of the content, was detrimental to the supercooling degree of the SAT-CNW nanocomposites. The non-polar nature, high specific surface area, and high aspect ratio of GNP made it a challenge to uniformly disperse them in the SAT matrix.

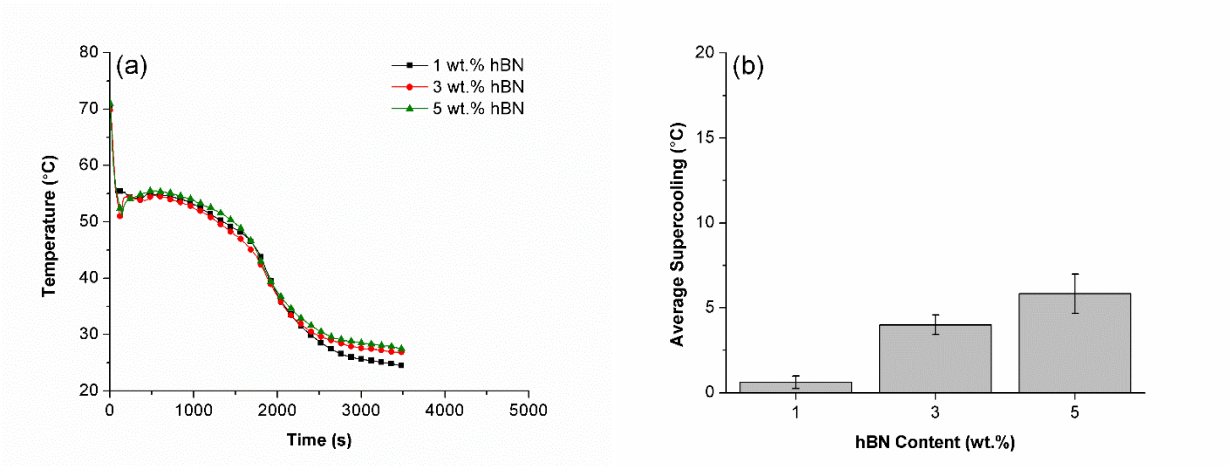

Figure 0.6. The freezing behaviors of SAT-CNW nanocomposites with different hBN contents: (a) Cooling curve; and (b) supercooling degrees

The porous space formed by the agglomeration of GNP would restrict the mobility of SAT molecules, and thereby limiting the aggregation and crystallization of SAT. Such observation was consistent with another study of SAT composites filled with expanded graphite as a heat transfer enhancer. Therefore, although GNP was an effective filler to promote the

nancomposite's effective thermal conductivity, the negative impact on the supercooling would limit its uses in SAT-based PCM.

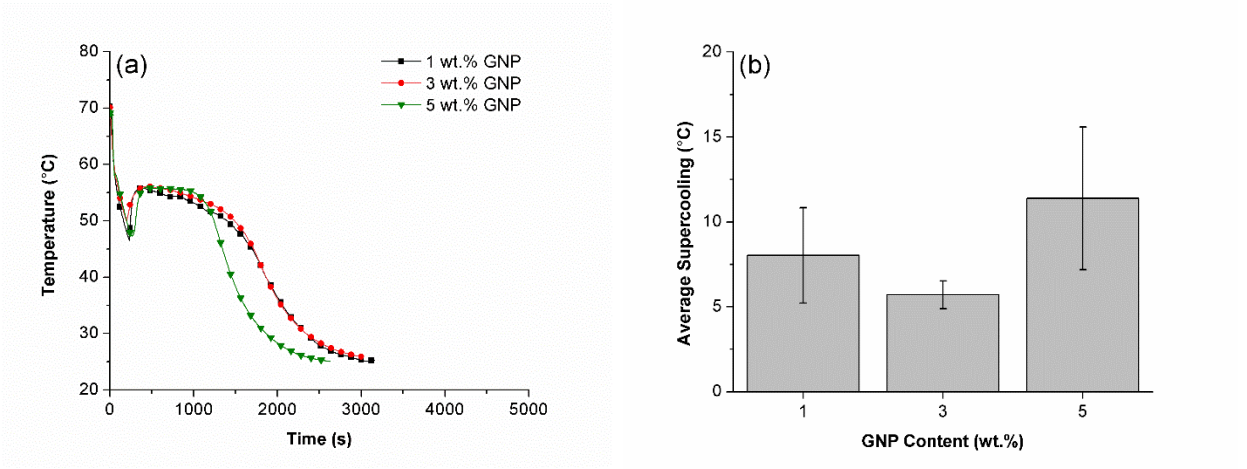

Figure 0.7. The freezing behaviors of SAT-CNW nanocomposites with different GNP contents: (a) Cooling curve; and (b) supercooling degrees

4.2.6. Thermal properties and thermal energy storage abilities of the SAT nanocomposites

Pure SAT and SAT nanocomposites fabricated with different formulations were analyzed by DSC to determine their melting temperatures and latent heat of fusion. Pure SAT's melting temperature and latent heat of fusion were 59°C and 258 $J \cdot g^{-1}$, respectively. The effects of different components on SAT's thermal properties are summarized in Table 0.3. By adding 1.0 wt.% CNW and 3.0 wt.% CMC as the nucleating agent and thickening agent, respectively, the latent heat of fusion dropped to 241 $J \cdot g^{-1}$. This could be attributed to the reduced mass fraction of SAT when CNW and CMC were added as SAT was the only component that contributed to the latent heat. The addition of thermally conductive nanofillers (i.e., hBN or GNP) further decreased the mass fraction of SAT in the nanocomposites. Therefore, as the hBN or GNP contents increased, the latent heat gradually decreased to approximately 210 $J \cdot g^{-1}$ when the filler

loadings reached 5 wt.%. Nevertheless, all the SAT-CNW nanocomposites prepared had their latent heat of fusion higher than 200 $J \cdot g^{-1}$, which were higher than that of the conventional paraffinic PCM (the paraffinic PCM latent heat ranges from 150 to 220 $J \cdot g^{-1}$ [8]).

Table 0.3. Thermal properties of pure SAT and SAT nanocomposites with different formulations

Sample	Enthalpy (J·g-1)	Melting Temp. (°C)
Pure SAT	257	59.1
Base Case	241	58.7
Base case + 1 wt.% hBN	234	60.0
Base case + 3 wt.% hBN	230	59.6
Base case + 5 wt.% hBN	210	58.6
Base case + 1 wt.% GNP	240	59.0
Base case + 3 wt.% GNP	224	59.8
Base case + 5 wt.% GNP	206	58.5

Unlike the heat of fusion, the melting temperatures of all samples were virtually unchanged. Furthermore, thermal cycling of the SAT-CNW nanocomposite with the base case formulation was conducted to investigate its thermal stability. It was observed that the nanocomposite maintained a low degree of supercooling and the heat of fusion was virtually unchanged after the sample had undergone 20 thermal cycles (the melting was conducted at 70°C).

4.3. Encapsulation of SAT with polylactic acid shell

Three different methods (i.e. water in oil in water, oil in water, solid in oil in water) were used to encapsulate the hydrophilic SAT in polylactic acid shell.

4.3.1. Material

PLA (Ingeo 8052D NatureWorks LLC) was used as the polymeric shell of the microPCM. SAT (Sigma Aldrich) was used as the PCM core. 87–89% hydrolyzed polyvinyl alcohol (PVA, Sigma Aldrich) with an average molecular weight of 146,000–186,000 g mol^{-1} and Brij52 (Sigma Aldrich, ReagentPlus grade) were used as emulsifiers. Dichloromethane (DCM, Caledon Laboratory Chemical), with the density of 1320 $kg \cdot m^{-3}$, was the organic solvent for the preparation of the oil phase. Deionized water was the aqueous medium. All materials and chemicals were used as received.

4.3.2. Preparation of PLA- SAT microcapsules

Microencapsulation of a PA core in a PLA shell was conducted by the different types of solvent evaporation methods, which will be described in following sections:

4.3.2.1 Water in oil in water

1.2 g of PLA was dissolved in 38.5 g of DCM to prepare the oil phase (O). The initial water phase (W1) was made by dissolving 1 g of SAT in 9 g of PVA 0.1% water solution. 4.81 g of W1 was added to 31.8 g of O and was sonicated for five minutes and the first emulsion is prepared. By using this formulation, the ratio of SAT core to PLA shell is 0.5. 10 g of first emulsion is added to 120 g of W2, which is 1 wt.% or 3 wt.% PVA solution in water (sample 1 and 2). This double emulsion is stirred at 300 rpm for 5 minutes and then heated at 45°C for one hour while being stirred at 250 rpm to evaporate the organic solvent. The final mixture is then centrifuged at 4000 rpm and the solid particles were collected and dried.

In another trial, 2 wt.% of Brij52 oil soluble surfactant was added to DCM to enhance the compatibility of oil phase and inner water phase. All the described steps were followed to prepare the microcapsules (sample 3).

4.3.2.2 Oil in water

In this method, a mixture of polar and non-polar solvents was chosen, so that they can dissolve both core and shell materials. 0.5 g of SAT was dissolved in 10 grams of methanol. 1.2 g of PLA was dissolved in 38.5 g of DCM. 3.2 g of SAT solution was added to 10 g of PLA solution to prepare the oil phase. This mixture was stirred for 5 minutes until a homogenous solution was obtained. 10 g of oil phase was added to 120 g of water phase which was a 3 wt.% PVA solution in water. This single emulsion is stirred at 300 rpm for 5 minutes and then heated at 45℃ for one hour while being stirred at 250 rpm to evaporate the organic solvent. The final mixture is then centrifuged at 4000 rpm and the solid particles were collected and dried (sample 4).

4.3.2.3 Solid in oil in water

1.2 g of PLA was dissolved in 38.5 g of DCM to prepare the oil phase (O). 0.3 gram of solid SAT was added to 10 grams of the oil phase. The mixture was stirred for 5 minutes at 300 rpm. This mixture was then added to 3% PVA solution in water. This mixture was stirred at 300 rpm for 5 minutes and then heated at 45 ℃ for one hour while being stirred at 250 rpm to evaporate the organic solvent. The final mixture is then centrifuged at 4000 rpm and the solid particles were collected and dried (sample 5).

4.3.3. Results and discussion

PLA–SAT microPCM fabricated by using different methods and material compositions were analyzed by DSC to compare their performances and operating temperatures for thermal energy storage. Pure SAT's melting temperature and latent heat of fusion were 59°C and 258 $J \cdot g^{-1}$, respectively. By comparing this with the latent heat of fusion of pure SAT using Equation 3.1, the core content of PLA– SAT microPCM can be calculated. The melting temperatures, the

enthalpies of fusion, and the core contents of different microPCM samples are summarized in Table 0.4.

Table 0.4. Thermal properties of PLA–PA microPCM

Sample	Enthalpy ($J \cdot g^{-1}$)	Melting Temp. (°C)	Core Content (%)
1	-	-	-
2	-	-	-
3	0.7	57	0.2
4	2.71	62	1
5	1.93	62	0.7

These results are in agreement with the pharmaceutical researches trying to encapsulate medicine for drug delivery systems, as mentioned in the literature review section. However, the above-mentioned core contents are not enough for thermal energy storage purposes. These results indicate that emulsification and solvent evaporation method is not a good technique for preparation inorganic PCM microcapsules.

4.4. Conclusion

This chapter demonstrated the high potential of using the bio-derived chitin nanowhisker (CNW) as an effective nucleating agent to suppress the supercooling of sodium acetate trihydrate (SAT). The effects of different formulations and parameters, including CNW content, initial heating temperature, surfactant content, SAT particle size, as well as thermally conductive filler type and content, on supercooling degrees of SAT-CNW nanocomposites were investigated. Experimental results indicated that the SAT-CNW nanocomposite consisting of 1 wt.% of CNW

with particle sizes smaller than 53 μm, 3 wt.% of carboxymethyl cellulose (CMC), and 0.25 wt.% of sodium dodecyl sulfate (SDS) had the lowest supercooling degree during freezing. The exceptional phase change performance of this SAT-CNW nanocomposite could be maintained when the temperature during the melting cycle was at 70°C or below, as well as over repeating thermal cycles. Although both hexagonal boron nitride (hBN) and graphene nanoplatelets (GNP) were effective in enhancing the effective thermal conductivity of SAT-CNW nanocomposites, adding GNP was detrimental to the suppression of SAT's supercooling due to its lower compatibility with SAT and CNW. In the case of hBN, adding 1 wt.% filler would increase the nanocomposite's effective thermal conductivity by 35% without compromising the low supercooling degree of the nanocomposite. It is believed that the hydroxyl and amino groups at the edge of hBN platelets played key roles in their compatibility with both SAT and CNW; however, the quantities of these functional groups were limited. Therefore, further increase in hBN loadings to 3 wt.% or beyond led to challenges in uniformly dispersing them in the nanocomposites, and thereby caused an increase in the nanocomposite's supercooling. Furthermore, thermal analyses using differential scanning calorimetry revealed that the addition of any external agent would decrease the SAT-CNW nanocomposite's heat of fusion proportionally without affecting their melting temperature. It was because SAT was the only component contributed to the energy storage and release. Nevertheless, all nanocomposites possessed excellent thermal energy storage capability when comparing to organic phase change materials.

Several experiments based on emulsification solvent evaporation method was performed to encapsulate the hydrophilic SAT with polymeric shell. The results were totally comparable to the

pharmaceutical research, however the core contents of the products were not enough for thermal energy storage purposes.

Chapter 5
Conclusion and Recommendations

5.1. Conclusion

Global warming and the necessity of cutting down on the consumption of non-renewable fossil fuels urge the governments to look for novel energy storage systems. Phase change materials can be a possible solution that enables thermal energy storage in many applications especially in solar cells, packaging, and building materials. When PCM undergo isothermal melting, sublimation or vaporization, energy is absorbed from the surrounding and saved in the material. In contrast, when PCM solidify or condense, energy is released. PCM needs to be covered or encapsulated during phase transition from solid to liquid to prevent migrating and reacting with the environment.

In this context, first, encapsulation of vegetable-derived PCM with bio-based polylactic acid shell by solvent evaporation and oil-in-water emulsification was investigated. Different parametric studies were conducted to investigate the effects of PCM and solvent content, oil phase-to-aqueous phase ratio, as well as surfactant type and content on the morphology, particle size, and thermal properties of the PCM microcapsules. Experimental results showed that PVA was a superior emulsifier to SDS in the emulsion systems being studied. There also existed an optimal PVA concentration to reduce the average size of microPCM. When the PVA concentration was above this optimal level, the emulsifier molecules tend to form micelles among themselves. This led to the adhesion of tiny microspheres on the surface of microPCM as well as larger microPCM. The findings of the first phase of this thesis revealed the possibility of producing 100% bio-based and thermally stable PCM microcapsules for the first time.

Second, an inorganic PCM, SAT, with a melting point similar to the bio-based organic PCM that was used in the first phase of the PCM was chosen. Inorganic phase change materials possess superior properties such as better thermal conductivity, higher latent heat of fusion, and lower price to their organic counterparts. However, their extreme supercooling during freezing and phase segregation during melting have led to challenges in their applications to thermal energy storage. A comprehensive parametric study revealed that many different factors such as nucleating agent content, PCM particle size, initial heating temperature, thermally conductive filler and surfactant content can affect the supercooling behavior of salt hydrate. An optimum balance between all of the mentioned parameters was found, and a thermally stable SAT nanocomposite was prepared. By adding 1 wt.% of hBN, the thermal conductivity of SAT enhanced for about 35% while low supercooling degree was not compromised. Three methods of single emulsion, double emulsion and S/O/W solvent evaporation were used to encapsulate the SAT in PLA. The results indicated that although the above-mentioned method can be proper for drug delivery purposes, however, their application for thermal energy storage is not recommended since the core content is not sufficient.

5.2. Recommendation for Future Work

This work focused on encapsulation of bio-based and inorganic PCM and also thermal tuning and supercooling prevention of inorganic PCM. The results showed that single and double emulsion solvent evaporation method is not a suitable technique to prepare inorganic PCM microcapsule since the core content of the product is not sufficient for thermal energy storage purposes.

For encapsulation of the inorganic PCM, one can use immersion of bio-based or synthetic polymeric foams in molten state SAT, so that the salt will be wrapped in the foam. The porous

structure of the foam can provide nucleation sites for the salt hydrate and hence decrease the supercooling degree of the salt. Also, the wrapped salt will not be dehydrated in multiple heating and cooling cycles. Encapsulation with hydrophilic polymers using polymerization method is another possible approach that needs to be more investigated in the future. By encapsulating the inorganic PCM, one can perform a thorough comparison between the thermal performance of organic and inorganic PCM microcapsule and composites.

Bibliography

[1] M. Anderson, Global warming, 1st ed., Britannica Educational Pub. in association with Rosen Educational Services, New York, 2012.

[2] M.M. Halmann, M. Steinberg, Greenhouse gas carbon dioxide mitigation : science and technology, 1st ed., Lewis Publishers, Boca Raton, 1999.

[3] J.K. Casper, Greenhouse gases : worldwide impacts, 1st ed., Facts On File, New York, 2010.

[4] P. Breeze, Greenhouse Gas Emissions and Power Generation, in: Electr. Gener. Environ., Elsevier, 2017: pp. 23–31.

[5] J.L. Moan, Z.A. Smith, Energy use worldwide: a reference handbook, ABC-CLIO, Santa Barbara, 2007.

[6] L. Barreto, A. Makihira, K. Riahi, The hydrogen economy in the 21st century: a sustainable development scenario, Int. J. Hydrogen Energy. 28 (2003) 267–284.

[7] B. Zalba, J.M. Marín, L.F. Cabeza, H. Mehling, Review on thermal energy storage with phase change: Materials, heat transfer analysis and applications, Appl. Therm. Eng. 23 (2003) 251–283.

[8] S.S. Chandel, T. Agarwal, Review of current state of research on energy storage, toxicity, health hazards and commercialization of phase changing materials, Renew. Sustain. Energy Rev. 67 (2017) 581–596.

[9] R. Jacob, F. Bruno, Review on shell materials used in the encapsulation of phase change materials for high temperature thermal energy storage, Renew. Sustain. Energy Rev. 48 (2015) 79–87.

[10] S.A. Mohamed, F.A. Al-Sulaiman, N.I. Ibrahim, M. Hasan Zahir, A. Al-Ahmed, R. Saidur, B. Yılbaş, A. Sahin, A review on current status and challenges of inorganic phase change materials for thermal energy storage systems, Renew. Sustain. Energy Rev. 70 (2017) 1072–1089.

[11] A. Sarı, A. Karaipekli, Thermal conductivity and latent heat thermal energy storage characteristics of paraffin/expanded graphite composite as phase change material, Appl. Therm. Eng. 27 (2007) 1271–1277.

[12] M.M. Kenisarin, Thermophysical properties of some organic phase change materials for latent heat storage. A review, Sol. Energy. 107 (2014) 553–575.

[13] H. Akeiber, P. Nejat, M.Z.A. Majid, M.A. Wahid, F. Jomehzadeh, I. Zeynali Famileh, J.K. Calautit, B.R. Hughes, S.A. Zaki, A review on phase change material (PCM) for sustainable passive cooling in building envelopes, Renew. Sustain. Energy Rev. 60 (2016) 1470–1497.

[14] B. Zalba, J.M. Marín, L.F. Cabeza, H. Mehling, Review on thermal energy storage with phase change: materials, heat transfer analysis and applications, Appl. Therm. Eng. 23 (2003) 251–283.

[15] P. SCHOSSIG, H. HENNING, S. GSCHWANDER, T. HAUSSMANN, Micro-encapsulated phase-change materials integrated into construction materials, Sol. Energy Mater. Sol. Cells. 89 (2005) 297–306.

[16] W. Kong, X. Fu, Z. Liu, C. Zhou, J. Lei, A facile synthesis of solid-solid phase change material for thermal energy storage, Appl. Therm. Eng. 117 (2017) 622–628.

[17] W.-D. Li, E.-Y. Ding, Preparation and characterization of cross-linking PEG/MDI/PE copolymer as solid–solid phase change heat storage material, Sol. Energy Mater. Sol. Cells. 91 (2007) 764–768.

[18] A. Sari, C. Alkan, A. Biçer, Synthesis and thermal properties of polystyrene-graft-PEG copolymers as new kinds of solid-solid phase change materials for thermal energy storage, Mater. Chem. Phys. 95 (2011) 3195–3201.

[19] A. Arora, Hydrocarbons (Alkanes, Alkenes And Alkynes), 1st ed., Discovery Publishing, New Delhi, 2012.

[20] H.S. Stoker, General, organic, and biological chemistry, 6th ed., Brooks Cole, Belmont, 2012.

[21] S.D. Sharma, K. Sagara, LATENT HEAT STORAGE MATERIALS AND SYSTEMS: A REVIEW, Int. J. Green Energy. 2 (2005) 1–56.

[22] S.D. Sharma, D. Buddhi, R.L. Sawhney, Accelerated thermal cycle test of latent heat-storage materials, Sol. Energy. 66 (1999) 483–490.

[23] A. Shukla, D. Buddhi, R.L. Sawhney, Thermal cycling test of few selected inorganic and organic phase change materials, Renew. Energy. 33 (2008) 2606–2614.

[24] F. Bettelheim, Introduction to Organic and Biochemistry, 8th ed., Nelson Education, Belmont, 2012.

[25] S.-G. Jeong, O. Chung, S. Yu, S. Kim, S. Kim, Improvement of the thermal properties of Bio-based PCM using exfoliated graphite nanoplatelets, Sol. Energy Mater. Sol. Cells. 117 (2013) 87–92.

[26] A. Sarı, K. Kaygusuz, Some fatty acids used for latent heat storage: thermal stability and corrosion of metals with respect to thermal cycling, Renew. Energy. 28 (2003) 939–948.

[27] M. Liu, W. Saman, F. Bruno, Review on storage materials and thermal performance enhancement techniques for high temperature phase change thermal storage systems, Renew. Sustain. Energy Rev. 16 (2012) 2118–2132.

[28] I. Dincer, M. a. Rosen, H.Ö. Paksoy, Thermal Energy Storage for Sustainable Energy Consumption, in: H.Ö. Paksoy (Ed.), Therm. Energy Storage Sustain. Energy Consum., Springer Netherlands, Dordrecht, 2007: pp. 177–192.

[29] H.W. Ryu, S.W. Woo, B.C. Shin, S.D. Kim, Prevention of supercooling and stabilization of inorganic salt hydrates as latent heat storage materials, Sol. Energy Mater. Sol. Cells. 27 (1992) 161–172.

[30] M. Jinfeng, D. Xian, H. Pumin, L. Huiliang, Preparation research of novel composite phase change materials based on sodium acetate trihydrate, Appl. Therm. Eng. J. 118 (2017) 817–825.

[31] B.M.L. Garay Ramirez, C. Glorieux, E.S. Martin Martinez, J.J.A. Flores Cuautle, Tuning of thermal properties of sodium acetate trihydrate by blending with polymer and silver

nanoparticles, Appl. Therm. Eng. 61 (2013) 838–844.

[32] A. Safari, R. Saidur, F.A. Sulaiman, Y. Xu, J. Dong, A review on supercooling of Phase Change Materials in thermal energy storage systems, Renew. Sustain. Energy Rev. 70 (2017) 905–919.

[33] T.M. Letcher, Storing Energy: with Special Reference to Renewable Energy Sources, illustrate, Elsevier, Amsterdam, 2016.

[34] J.R. Versey, S. Phongikaroon, M.F. Simpson, SEPARATION OF CsCl FROM LiCl-CsCl MOLTEN SALT BY COLD FINGER MELT CRYSTALLIZATION, Nucl. Eng. Technol. 46 (2014) 395–406.

[35] J. Mao, P. Hou, R. Liu, F. Chen, X. Dong, Preparation and thermal properties of SAT-CMC-DSP/EG composite as phase change material, Appl. Therm. Eng. 119 (2017) 585–592.

[36] E.C. Guyer, D.L. Brownell, Handbook of applied thermal design, reprint, Taylor & Francis, Philadelphia, 1999.

[37] G. Lane, Phase change materials for energy storage nucleation to prevent supercooling, Sol. Energy Mater. Sol. Cells. 27 (1992) 135–160.

[38] P. Hu, D.-J. Lu, X.-Y. Fan, X. Zhou, Z.-S. Chen, Phase change performance of sodium acetate trihydrate with AlN nanoparticles and CMC, Sol. Energy Mater. Sol. Cells. 95 (2011) 2645–2649.

[39] W. Cui, Y. Yuan, L. Sun, X. Cao, X. Yang, Experimental studies on the supercooling and melting/freezing characteristics of nano-copper/sodium acetate trihydrate composite phase change materials, Renew. Energy. 99 (2016) 1029–1037.

[40] A. Sharma, S. Kumar kar, Energy Sustainability Through Green Energy, Springer India, New Delhi, 2015.

[41] G. Li, Y. Hwang, R. Radermacher, H.H. Chun, Review of cold storage materials for subzero applications, Energy. 51 (2013) 1–17.

[42] A. Sari, A. Onal, Thermal properties and thermal reliability of eutectic mixtures of some

fatty acids as latent heat storage materials, Energy Convers. Manag. 45 (2004) 365–376.

[43] K. Nagano, K. Ogawa, T. Mochida, K. Hayashi, H. Ogoshi, Thermal characteristics of magnesium nitrate hexahydrate and magnesium chloride hexahydrate mixture as a phase change material for effective utilization of urban waste heat, Appl. Therm. Eng. 24 (2004) 221–232.

[44] P.B. Salunkhe, P.S. Shembekar, A review on effect of phase change material encapsulation on the thermal performance of a system, Renew. Sustain. Energy Rev. 16 (2012) 5603–5616.

[45] M. Medrano, M.O. Yilmaz, M. Nogués, I. Martorell, J. Roca, L.F. Cabeza, Experimental evaluation of commercial heat exchangers for use as PCM thermal storage systems, Appl. Energy. 86 (2009) 2047–2055.

[46] R. Jacob, F. Bruno, Review on shell materials used in the encapsulation of phase change materials for high temperature thermal energy storage, Renew. Sustain. Energy Rev. 48 (2015) 79–87.

[47] W. Li, X. Zhang, X. Wang, G. Tang, H. Shi, Fabrication and morphological characterization of microencapsulated phase change materials (MicroPCMs) and macrocapsules containing MicroPCMs for thermal energy storage, Energy. 38 (2012) 249–254.

[48] R. Fioretti, P. Principi, B. Copertaro, A refrigerated container envelope with a PCM (Phase Change Material) layer: Experimental and theoretical investigation in a representative town in Central Italy, Energy Convers. Manag. 122 (2016) 131–141.

[49] W.-L. Cheng, B.-J. Mei, Y.-N. Liu, Y.-H. Huang, X.-D. Yuan, A novel household refrigerator with shape-stabilized PCM (Phase Change Material) heat storage condensers: An experimental investigation, Energy. 36 (2011) 5797–5804.

[50] A. Jamekhorshid, S.M. Sadrameli, M. Farid, A review of microencapsulation methods of phase change materials (PCMs) as a thermal energy storage (TES) medium, Renew. Sustain. Energy Rev. 31 (2014) 531–542.

[51] R. Dubey, T.C. Shami, K.U. Bhasker Rao, Microencapsulation technology and

applications, Def. Sci. J. 59 (2009) 82–95.

[52] J. Rodríguez, M.J. Martín, M.A. Ruiz, B. Clares, Current encapsulation strategies for bioactive oils: From alimentary to pharmaceutical perspectives, Food Res. Int. 83 (2016) 41–59.

[53] L. Sánchez, P. Sánchez, A. de Lucas, M. Carmona, J.F. Rodríguez, Microencapsulation of PCMs with a polystyrene shell, Colloid Polym. Sci. 285 (2007) 1377–1385.

[54] Y. Ma, X. Chu, W. Li, G. Tang, Preparation and characterization of poly(methyl methacrylate-co-divinylbenzene) microcapsules containing phase change temperature adjustable binary core materials, Sol. Energy. 86 (2012) 2056–2066.

[55] Y. Jiang, D. Wang, T. Zhao, Preparation, characterization, and prominent thermal stability of phase-change microcapsules with phenolic resin shell andn-hexadecane core, J. Appl. Polym. Sci. 104 (2007) 2799–2806.

[56] W. Li, G. Song, S. Li, Y. Yao, G. Tang, Preparation and characterization of novel MicroPCMs (microencapsulated phase-change materials) with hybrid shells via the polymerization of two alkoxy silanes, Energy. 70 (2014) 298–306.

[57] M. Li, M. Chen, Z. Wu, Enhancement in thermal property and mechanical property of phase change microcapsule with modified carbon nanotube, Appl. Energy. 127 (2014) 166–171.

[58] D.C. Hyun, N.S. Levinson, U. Jeong, Y. Xia, Emerging Applications of Phase-Change Materials (PCMs): Teaching an Old Dog New Tricks, Angew. Chemie Int. Ed. 53 (2014) 3780–3795.

[59] R.P. Patel, M.P. Patel, A.M. Suthar, Spray Drying Technology: an overview, Indian J. Sci. Technol. 2 (2009) 44–47.

[60] A. Sosnik, K.P. Seremeta, Advantages and challenges of the spray-drying technology for the production of pure drug particles and drug-loaded polymeric carriers, Adv. Colloid Interface Sci. 223 (2015) 40–54.

[61] M.N.A. Hawlader, M.S. Uddin, M.M. Khin, Microencapsulated PCM thermal-energy

storage system, Appl. Energy. 74 (2003) 195–202.

[62] R.H. Staff, K. Landfester, D. Crespy, Recent Advances in the Emulsion Solvent Evaporation Technique for the Preparation of Nanoparticles and Nanocapsules, in: Springer International Publishing, 2013: pp. 329–344.

[63] M. Li, O. Rouaud, D. Poncelet, Microencapsulation by solvent evaporation: state of the art for process engineering approaches., Int. J. Pharm. 363 (2008) 26–39.

[64] C. Anandharamakrishnan, Liquid-Based Nanoencapsulation Techniques, in: Springer New York, 2014: pp. 29–41.

[65] M. Iqbal, N. Zafar, H. Fessi, A. Elaissari, Double emulsion solvent evaporation techniques used for drug encapsulation, Int. J. Pharm. 496 (2015) 173–190.

[66] L.L. Schramm, E.N. Stasiuk, 2 Surfactants and their applications, Annu. Rep. Prog. Chem., Sect. C Phys. Chem. 99 (2003) 3–48.

[67] G. Kume, M. Gallotti, G. Nunes, Review on Anionic/Cationic Surfactant Mixtures, J. Surfactants Deterg. 11 (2008) 1–11.

[68] A.M. Grumezescu, A. Ficai, Nanostructures for Cancer Therapy, 1st ed., Elsevier, Amsterdam, 2017.

[69] I. Johansson, P. Somasundaran, Handbook for cleaning/decontamination of surfaces, 1st ed., Elsevier, Amsterdam, 2007.

[70] D. Ghosh, A.K. Pradhan, S. Mondal, N.A. Begum, D. Mandal, Proton transfer reactions of 4′-chloro substituted 3-hydroxyflavone in solvents and aqueous micelle solutions, Phys. Chem. Chem. Phys. 16 (2014) 8594.

[71] J. Wang, K. Sun, J. Wang, Y. Guo, Preparation of PLA-Coated Energy Storage Microcapsules and Its Application in Polyethylene Composites, Polym. Plast. Technol. Eng. 52 (2013) 1235–1241.

[72] A. Gaignaux, J. Réeff, F. Siepmann, J. Siepmann, C. De Vriese, J. Goole, K. Amighi, Development and evaluation of sustained-release clonidine-loaded PLGA microparticles, Int. J. Pharm. 437 (2012) 20–28.

[73] L. Al Haushey, M.A. Bolzinger, C. Bordes, J.Y. Gauvrit, S. Briançon, Improvement of a bovine serum albumin microencapsulation process by screening design, Int. J. Pharm. 344 (2007) 16–25.

[74] O. Karal-Yilmaz, M. Serhatli, K. Baysal, B.M. Baysal, Preparation and in vitro characterization of vascular endothelial growth factor (VEGF)-loaded poly(D,L-lactic-co-glycolic acid) microspheres using a double emulsion/solvent evaporation technique, J. Microencapsul. 28 (2011) 46–54.

[75] Vahid Haddadi Asl, Principles of Polymerization Engineering- Volume I: Polymer Technology, 7th ed., Amirkabir University of Technology Publication, Tehran, 2016.

[76] R. Arshady, Suspension, emulsion, and dispersion polymerization: A methodological survey, Colloid Polym. Sci. 270 (1992) 717–732.

[77] E. Vivaldo-Lima, P.E. Wood, A.E. Hamielec, A. Penlidis, An Updated Review on Suspension Polymerization, Ind. Eng. Chem. Res. 36 (1997) 939–965.

[78] L. Sánchez-Silva, J.F. Rodríguez, A. Romero, A.M. Borreguero, M. Carmona, P. Sánchez, Microencapsulation of PCMs with a styrene-methyl methacrylate copolymer shell by suspension-like polymerisation, Chem. Eng. J. 157 (2010) 216–222.

[79] C. Anandharamakrishnan, S.P. Ishwarya, Spray Drying Techniques for Food Ingredient Encapsulation, 1st ed., Wiley, Chichester, 2015.

[80] M. Khemani, M. Sharon, M. Sharon, Encapsulation of Berberine in Nano-Sized PLGA Synthesized by Emulsification Method, ISRN Nanotechnol. 2012 (2012) 1–9.

[81] L. Sánchez-Silva, J.F. Rodríguez, P. Sánchez, Influence of different suspension stabilizers on the preparation of Rubitherm RT31 microcapsules, Colloids Surfaces A Physicochem. Eng. Asp. 390 (2011) 62–66.

[82] X. Qiu, G. Song, X. Chu, X. Li, G. Tang, Preparation, thermal properties and thermal reliabilities of microencapsulated n-octadecane with acrylic-based polymer shells for thermal energy storage, Thermochim. Acta. 551 (2013) 136–144.

[83] G. Odian, Principles of Polymerization, John Wiley & Sons, Inc., Hoboken, NJ, USA,

2004.

[84] A. Sarı, C. Alkan, A. Biçer, A. Altuntaş, C. Bilgin, Micro/nanoencapsulated n-nonadecane with poly(methyl methacrylate) shell for thermal energy storage, Energy Convers. Manag. 86 (2014) 614–621.

[85] A. Sarı, C. Alkan, A.N. Özcan, Synthesis and characterization of micro/nano capsules of PMMA/capric–stearic acid eutectic mixture for low temperature-thermal energy storage in buildings, Energy Build. 90 (2015) 106–113.

[86] P.W. Morgan, Morgan, P. W., Interfacial Polymerization, in: Encycl. Polym. Sci. Technol., John Wiley & Sons, Inc., Hoboken, NJ, USA, 2011.

[87] J.W. Gooch, Interfacial Polymerization, in: Encycl. Dict. Polym., Springer New York, New York, NY, 2011: pp. 392–392.

[88] S. Zhan, S. Chen, L. Chen, W. Hou, Preparation and characterization of polyurea microencapsulated phase change material by interfacial polycondensation method, Powder Technol. 292 (2016) 217–222.

[89] M.J.T. Raaijmakers, N.E. Benes, Current trends in interfacial polymerization chemistry, Prog. Polym. Sci. 63 (2016) 86–142.

[90] S. Yu, S.-G. Jeong, O. Chung, S. Kim, Bio-based PCM/carbon nanomaterials composites with enhanced thermal conductivity, Sol. Energy Mater. Sol. Cells. 120 (2014) 549–554.

[91] T. Oya, T. Nomura, M. Tsubota, N. Okinaka, T. Akiyama, Thermal conductivity enhancement of erythritol as PCM by using graphite and nickel particles, Appl. Therm. Eng. 61 (2013) 825–828.

[92] H. Ji, Enhanced thermal conductivity of phase change materials with ultrathin-graphite foams for thermal energy storage, Energy Environ. Sci. 7 (2014) 1185.

[93] Z. Chen, J. Wang, Preparation and properties of graphene oxide-modified poly(melamine-formaldehyde) microcapsules containing phase change material n-dodecanol for thermal energy storage, J. Mater. Chem. A. 3 (2015) 11624–11630.

[94] F.A. Farret, M.G. Simões, Integration of renewable sources of energy, 2nd ed., Wiley,

Hoboken, 2017.

[95] F. Souayfane, F. Fardoun, P.-H. Biwole, Phase change materials (PCM) for cooling applications in buildings: A review, Energy Build. 129 (2016) 396–431.

[96] Advanced Phase Change Materials (PCM) Market | Industry Report 2020, 2014.

[97] R. Velraj, A. Pasupathy, Phase Change Material Based Thermal Storage for Energy Conservation in Building Architecture, Source. 7 (2005) 147–159.

[98] S. Mondal, Phase change materials for smart textiles - An overview, Appl. Therm. Eng. 28 (2008) 1536–1550.

[99] E. Oró, A. De Gracia, L.F. Cabeza, Active phase change material package for thermal protection of ice cream containers, Int. J. Refrig. 36 (2013) 102–109.

[100] RGEES | Manufacturer of PCM Based Temperature Controlled Packaging Systems for Transporting Medical Specimens, Blood products, Vaccine, Pharma and Life Science Products., (2017).

[101] P. Zhai, X.B. Chen, D.J. Schreyer, PLGA/alginate composite microspheres for hydrophilic protein delivery, Mater. Sci. Eng. C. 56 (2015) 251–259.

[102] B. Smith, Fundamentals of Fourier Transform Infrared Spectroscopy, (1996).

[103] G. Fang, H. Li, Z. Chen, X. Liu, Preparation and properties of palmitic acid/SiO2 composites with flame retardant as thermal energy storage materials, Sol. Energy Mater. Sol. Cells. 95 (2011) 1875–1881.

[104] S. Yang, Z.-H. Wu, W. Yang, M.-B. Yang, Thermal and mechanical properties of chemical crosslinked polylactide (PLA), Polym. Test. 27 (2008) 957–963.

[105] G. Höhne, W. Hemminger, H.-J. Flammersheim, Differential Scanning Calorimetri: An introduction for practitioners, Springer, Berlin, 1996.

[106] Q. Xu, A. Crossley, J.A.N. Czernuszka, Preparation and Characterization of Negatively Charged Poly (Lactic- co -Glycolic Acid) Microspheres, J. Am. Pharm. Assoc. 98 (2009) 2377–2389.

[107] J.. Shaeiwitz, A..-C. Chan, E.. Cussler, D.. Evans, The mechanism of solubilization in detergent solutions, J. Colloid Interface Sci. 84 (1981) 47–56.

[108] J.I. Goldstein, D.E. Newbury, P. Echlin, D.C. Joy, C.E. Lyman, E. Lifshin, L. Sawyer, J.R. Michael, Scanning Electron Microscopy and X-ray Microanalysis, 3rd ed., Springer, New York, 2012.

[109] V.K. Thakur, M.K. Thakur, Handbook of Polymers for Pharmaceutical Technologies, Wiley, Hoboken, 2015.

[110] H.-C. Chang, Y.-Y. Lin, C.-S. Chern, S.-Y. Lin, Determination of Critical Micelle Concentration of Macroemulsions and Miniemulsions, Langmuir. 14 (1998) 6632–6638.

[111] A. Kaizawa, N. Maruoka, A. Kawai, H. Kamano, T. Jozuka, T. Senda, T. Akiyama, Thermophysical and heat transfer properties of phase change material candidate for waste heat transportation system, Heat Mass Transf. 44 (2008) 763–769.

[112] P.J. Cullen, R.J. Romañach, N. Abatzoglou, C.D. Rielly, Pharmaceutical Blending and Mixing, illustrate, Wiley, Chichester, 2015.

[113] H.S. Kim, H.S. Bae, J. Yu, S.Y. Kim, Thermal conductivity of polymer composites with the geometrical characteristics of graphene nanoplatelets, Sci. Rep. 6 (2016) 26825.

[114] K. Sato, H. Horibe, T. Shirai, Y. Hotta, H. Nakano, H. Nagai, K. Mitsuishi, K. Watari, Thermally conductive composite films of hexagonal boron nitride and polyimide with affinity-enhanced interfaces, J. Mater. Chem. 20 (2010) 2749–2752.